Energy Reports 9 (2023) 1029–1053

Contents lists available at ScienceDirect

Energy Reports

journal homepage: www.elsevier.com/locate/egyr

Research paper

An efficient and reliable scheduling algorithm for unit commitment scheme in microgrid systems using enhanced mixed integer particle swarm optimizer considering uncertainties

M. Premkumar [a,*], R. Sowmya [b], C. Ramakrishnan [c], Pradeep Jangir [d], Essam H. Houssein [e], Sanchari Deb [f,*], Nallapaneni Manoj Kumar [g,h,i,**]

[a] Department of Electrical and Electronics Engineering, Dayananda Sagar College of Engineering, Bengaluru 560078, Karnataka, India
[b] Department of Electrical and Electronics Engineering, National Institute of Technology, Tiruchirappalli 620015, Tamil Nadu, India
[c] Department of Electrical and Electronics Engineering, SNS College of Technology, Coimbatore 641035, Tamil Nadu, India
[d] Rajasthan Rajya Vidyut Prasaran Nigam, Sikar 332025, Rajasthan, India
[e] Faculty of Computers and Information, Minia University, Minia, Egypt
[f] School of Engineering, University of Warwick, Coventry CV4 7AL, UK
[g] School of Energy and Environment, City University of Hong Kong, Kowloon, Hong Kong
[h] Center for Research and Innovation in Science, Technology, Engineering, Arts, and Mathematics (STEAM) Education, HICCER – Hariterde International Council of Circular Economy Research, Palakkad 678631, Kerala, India
[i] Department of Electrical Engineering, Graphic Era (Deemed to be University), Dehradun 248002, Uttarakhand, India

ARTICLE INFO

Article history:
Received 27 August 2022
Received in revised form 7 November 2022
Accepted 7 December 2022
Available online xxxx

Keywords:
Battery energy storage
Microgrids
Mixed integer algorithm
Particle swarm optimizer
Uncertainties
Unit commitment

ABSTRACT

The use of an electrical energy storage system (EESS) in a microgrid (MG) is widely recognized as a feasible method for mitigating the unpredictability and stochastic nature of sustainable distributed generators and other intermittent energy sources. The battery energy storage (BES) system is the most effective of the several power storage methods available today. The unit commitment (UC) determines the number of dedicated dispatchable distributed generators, respective power, the amount of energy transferred to and absorbed from the microgrid, as well as the power and influence of EESSs, among other factors. The BES deterioration is considered in the UC conceptualization, and an enhanced mixed particle swarm optimizer (EMPSO) is suggested to solve UC in MGs with EESS. Compared to the traditional PSO, the acceleration constants in EMPSO are exponentially adapted, and the inertial weight in EMPSO decreases linearly during each iteration. The proposed EMPSO is a mixed integer optimization algorithm that can handle continuous, binary, and integer variables. A part of the decision variables in EMPSO is transformed into a binary variable by introducing the quadratic transfer function (TF). This paper also considers the uncertainties in renewable power generation, load demand, and electricity market prices. In addition, a case study with a multiobjective optimization function with MG operating cost and BES deterioration defines the additional UC problem discussed in this paper. The transformation of a single-objective model into a multiobjective optimization model is carried out using the weighted sum approach, and the impacts of different weights on the operating cost and lifespan of the BES are also analyzed. The performance of the EMPSO with quadratic TF (EMPSO-Q) is compared with EMPSO with V-shaped TF (EMPSO-V), EMPSO with S-shaped TF (EMPSO-S), and PSO with S-shaped TF (PSO-S). The performance of EMPSO-Q is 15%, 35%, and 45% better than EMPSO-V, EMPSO-S, and PSO-S, respectively. In addition, when uncertainties are considered, the operating cost falls from $8729.87 to $8986.98. Considering BES deterioration, the BES lifespan improves from 350 to 590, and the operating cost increases from $8729.87 to $8917.7. Therefore, the obtained results prove that the EMPSO-Q algorithm could effectively and efficiently handle the UC problem.

* Corresponding authors.
** Corresponding author at: School of Energy and Environment, City University of Hong Kong, Kowloon, Hong Kong.
E-mail addresses: mprem.me@gmail.com (M. Premkumar), sowmyanitt@gmail.com (R. Sowmya), ramramki.krishnan@gmail.com (C. Ramakrishnan), pkjmtech@gmail.com (P. Jangir), esam.halim@fci.bu.edu.eg (E.H. Houssein), sanchari.deb@warwick.ac.uk (S. Deb), mnallapan2-c@my.cityu.edu.hk (N.M. Kumar).

https://doi.org/10.1016/j.egyr.2022.12.024

1. Introduction

Power system operational planning models integrate new distributed energy resources (DERs), with most such systems being Microgrids (MGs) (Alsaidan et al., 2018; Gilani et al., 2020). An MG can be defined as a system that incorporates DERs such as electrical energy storage systems (EESS), tiny wind turbine systems, combined heat and power units, photovoltaic systems, and interruptible loads and is configured in such a direction where it has at least one configurable source of energy (Moncecchi et al., 2020; Ahmadi et al., 2015; Khorramdel et al., 2016). The rising integration of such DERs has led to more difficult activities such as demand-side management, peak shaving, price and loss reduction, and operational planning becoming more difficult to do (Deckmyn et al., 2017). The MG operator schedules its dispatchable resources most effectively, considering the uncertainties in unreliable energy production, power market rate, and interruptible loads. Integrating renewable distributed generating units into the grid using MGs to do it effectively is possible. Renewable distributed generation provides unpredictable and inconsistent energy, and it creates new challenges for MGs (Mahmoud, 2017; Jadhav et al., 2019; Choudhury, 2020; Invernizzi and Vielmini, 2018).

Diverse solutions are employed to reduce the unpredictability and intermittent nature of sustainable distributed generation (DG). To sustain the frequency and voltage of the MG for both short- and long-term operations, the EESSs are crucial components of the system. The EESS is a critical component in integrating DG into the MG (Khorramdel et al., 2016; Khalid et al., 2021; Rezaee Jordehi, 2021a; Ferinar and Masoud, 2018). Different energy storage methods have been used at the turbine and farm stages for offshore wind to balance power fluctuation and enable wind energy to be more interoperable with utilities and MGs (Gao, 2015; Faisal et al., 2018). It is being recommended and explored that an alternative configuration for photovoltaic converters be developed to integrate batteries into photovoltaic to make them able to produce constant power on overcast days (Premkumar and Sowmya, 2019). The use of an EESS is often considered to be the most effective method among these. EESS can store surplus renewable power for use at a later stage when it is more beneficial, either from a financial or technical standpoint. EESS is utilized for various purposes, including cost reduction, frequency, and voltage stability improvement, power quality improvement, energy exchange, and deferment of capital expenses. In terms of EESS, battery energy storage (BES) is regarded as the most promising choice due to its sophistication and capacity to provide high power density simultaneously (Chen and Liu, 2021; Chaudhary et al., 2021).

Lithium-ion technology and numerous other technologies have supplanted the lead-acid technology that was previously in use. There are various types of EESS today, each with its properties, such as high energy density, effectiveness, price, longevity, and fast response (Moncecchi et al., 2018). Flow batteries, fuel cells, pumped hydro, pressurized air, ultracapacitors, flywheels, and superconducting magnetic EESSs are all examples of EESSs (Alvarado-Barrios et al., 2020). Currently, EESSs are installed in the majority of MGs. Several efforts have been undertaken to improve the efficiency of the deployment of EESSs to MGs in MG planning. Research is currently being conducted to determine the appropriate size and position for energy storage within an MG to achieve the lowest possible price and network power losses while simultaneously increasing the reliability and certainty of the MG (Lacap et al., 2021; Gaurav et al., 2015; Hittinger et al., 2015; Huang and Yang, 2021).

Microgrids are provided with energy management systems (EMSs) to keep operating costs and carbon emissions minimum. Economic load dispatch and UC are the two primary elements of the EMS (Alvarado-Barrios et al., 2019; Rodríguez del Nozal et al., 2020; Trivedi et al., 2016). When using the demand, UC module and DER information have been sent to the MG central controller, and the set of highly dedicated dispatchable distributed generations with their power, the power imported/exported from/to the grid, and the position and power of EESS devices are ascertained (Jangir et al., 2017). In contrast, all associated constraints of the microgrid are comfortable, and the set of dedicated dispatchable DGs. Due to the uncertainty in forecasting demand, renewable energy, and market rate, UC in EESS incorporated MGs is modeled as a limited, mixed binary continuous problem with unknown input data. The literature has proposed modeling and solving UC in EESS-integrated MGs using various optimization strategies (Alsaidan et al., 2017).

The authors of Murty and Kumar (2020) suggested an optimal energy dispatch approach for standalone and grid-connected microgrids using DERs, including EESS. Techno-economic implications of hybrid energy systems. The authors have addressed the problem thus far to reduce operating costs. For efficient energy management of MGs, power losses and emission-related objectives are also addressed. A new multiobjective solution for EMS together with a demand response (DR) program. Its influence on optimal energy dispatch and techno-commercial benefits are also included in the optimization problem. A fuzzy interface was also created for EESS scheduling. The authors of Sufyan et al. (2019) discover that economical scheduling considers the optimal battery capacity in isolated microgrids, resulting in lower operational costs. Extreme discharge, on the other hand, reduces the battery's longevity. As a result, the price of real-time battery operation is calculated by considering the depth of discharge at every iteration cycle. The firefly method also optimizes the economic schedule with battery sizing. To enable battery swap station existence as an acceptable solution for electric vehicle requirement problems, the authors of Ferinar and Masoud (2018) would go into considerable detail. Accordingly, the problem has intersected with two tiers of an operational field in this regard. In addition, issues about the battery's longevity would be considered as a major component in the decision-making process for two different scenario scenarios. It is an appropriate answer for governments that have been unsuccessful in implementing electric vehicles in their respective territories.

According to the researchers of Khorramdel et al. (2016), they are attempting to examine the UC problem based on a here-and-now (HN) strategy and cost–benefit analysis for the appropriate size of battery banks (BBs) and MGs that are powered by wind energy conversion systems. The particle swarm optimization (PSO) algorithm addresses this problem to decrease the overall cost while simultaneously increasing the total benefits. BBs and non-BBs scenarios have indeed been studied in this article in two operating configurations: (1) grid-connected and (2) standalone. Twelve operating situations have been examined in the existence and absence of BBs. According to the HN strategy, wind power unpredictability is applied as a limitation in such operating modes. The authors explain the mathematical equations associated with the HN technique in MGs and its integration into a UC problem to determine the optimal size of BBs. The impact of sustainable power and the availability of electric vehicles on unit commitment is investigated (Zhu et al., 2022). It has been decided to use a new parallel social learning PSO algorithm. The suggested model is tested on various UC problems in several different circumstances. It has been shown that renewables and electric vehicles can help to alleviate the stress on the grid.

The authors of Li et al. (2021) discussed the difference between traditional Seng-Cheol Kang and multi-band uncertainty robust optimization techniques. A linear UC model that considers wind power unpredictability is developed based on the

robust optimization model of the multi-band uncertainties. It is recommended that a parameter selection technique for a multi-band uncertainties resilient optimization method be used in conjunction with empirical datasets of wind power. The authors also compare and analyze the resilience and economy of UC in traditional, Seng-Cheol Kang, and multi-band uncertainty robust optimization techniques as three different approaches to problem-solving under uncertainty. The authors of Wang et al. (2021) study consider the UC scheme and solve multidimensional energy trading problems (ETPs). The first step is to develop a mixed-integer quadratic programming (MIQP) framework that can be used to define UC for every MG and energy exchange between multiple MGs. In the following step, binary parameters from UC problems are eased to persuade the non-convex model into an amenable convex model. It is also recommended to use an alternating optimization technique built on the alternate direction method of multipliers (ADMM) and the MIQP block to simultaneously handle continuous and binary variables. An in-depth rounding-off technique using thresholds is created to deal with generators that are out of bounds, smooth the variable transfer between the ADMM and MIQP blocks, and provide convergence evidence. The authors of Hong et al. (2022) have handled the UC problem using chance-constrained goal programming, and the energy storage system is also taken into account the UC problem.

The authors of Sayed et al. (2021) recommended a hybrid technique to solve the UC problem under stochastic and deterministic load demand. This technique comprises PSO and an equilibrium optimizer. However, the authors considered the UC problem as a continuous optimization problem. The author of Rezaee Jordehi (2021b, 2020a) suggested a modified PSO by utilizing the quadratic transfer function to solve the UC problem of the microgrid. Various case studies are considered to validate the suggested strategy; however, the algorithm is not tested with various other transfer functions. The authors of Mohammadi and Mohammadi (2014) discussed the difficulty of achieving the best possible performance of a microgrid in the presence of uncertainty. It is proposed that an EESS operate at its most efficient, and the approach ensures that the operation is feasible in most circumstances. The resultant optimization model is represented as a mixed-integer linear programming (MILP) with a quadratic cost function. A UC framework for micro-grid based on the fuel cell as EESS was proposed by the authors of Mohammadi and Mohammadi (2014) and solved using an enhanced cuckoo search algorithm. Hydrogen storage control is implemented to make the possible use of many fuel cells. It is necessary to utilize a scenario-based stochastic optimization model since the nature of the load, photovoltaic, wind turbine output power, and market pricing is unknown. The optimal size of energy storage devices is also discussed. The authors of Marzband et al. (2017) investigated sustainable day-ahead planning of grid-connected MG incorporating dispatchable distributed energy resources and adaptable load demand, specifically investigating the synchronously existing controllable and uncontrollable resources available despite the availability of responsive and non-responding loads. It also presents an efficient energy management system optimization algorithm based on MILP and the GAMS deployment for generating power optimization with the lowest possible hourly power system operating expense and the most sustainable power generation. The UC of MG with wind power considering multi-time scale demand response was discussed in Xu et al. (2021) and the MILP was used to solve the UC problem. The optimal scheduling of UC considering the electric vehicles and renewable power generation uncertainties is discussed in Pan and Liu (2022) and the authors have used the CPLEX solver to handle the UC problem.

The authors of Aghdam et al. (2020) recommended that a systematic multi-layer method for UC in multiple MG systems, comprising renewable power units and battery energy storage, has been developed. When it comes to the first layer, every MG is responsible for its regional day-ahead scheduling and determining whether it has excess or deficiency power. The next layer is where the MG operator gathers data from various microgrids and performs a global optimization, and the other layer is where microgrids are responsible for a deferment based on orders obtained from the MG operator. When dealing with the problem's constraints, chance-constrained computing has been applied; nevertheless, the uncertainty of load demand and renewable energy production has still not been considered. The authors of Kim et al. (2020) considered the problem of UC in an EESS-integrated MG with combined heat power, photovoltaic, and wind generators as mixed-integer non-linear programming, with MG system constraints and reactive power dispatch, has taken into account, and parallel benders decomposition-based optimization methodology has been employed to solve same. On the other hand, the uncertainties associated with demand and renewable energy production have still not been considered. In order to utilize each generator's features to their highest extent, lower energy costs, decrease the impact of carbon dioxide emissions, and raise the incorporation of the microgrid into energy systems, management strategies for complex energy systems composed of various technologies are essential. Therefore, the authors of Nicolosi et al. (2021) have reported a new MILP method to compute the management of microgrid systems.

The functioning of BES has a considerable impact on the longevity and deterioration of the network. The depth to which it is discharged and the number of discharging/charging events it undergoes significantly impact BES deterioration. Because of the cyclic deterioration of BES, it may need to be changed before its stated life span is completed. The lifetime of BES diminishes as the depth of discharge (DoD) of the system is increased (Alsaidan et al., 2018; Bao et al., 2021; Abdulgalil et al., 2019). The key findings must be addressed in relation to the findings that have been evaluated. Ignoring that the DoD impacts the lifespan and operational costs of BES, it has not been addressed in most UC for MGs. The risks associated with load demand, photovoltaic or wind power generation, and market price have still not been considered in certain circumstances (Tiwari et al., 2021; Abujarad et al., 2017). In UC, neglecting all or some ambiguous facts makes it impossible to make realistic decisions. Considering the sophistication of metaheuristic optimization algorithms, these have only been applied in a limited number of EESS-integrated MGs to solve UC problems. In addition, the emission factor has not been solved while handling the UC problem in many research works (Tiwari et al., 2018; Jiao et al., 2017; Lijun et al., 2021; Kumar, 2021).

After thorough investigation, this paper introduces BES deterioration along with an effective optimization algorithm to solve UC in battery storage-integrated grid-tied MGs while considering and dealing with the sources of uncertainty of load demand, market demand price, and renewable energy production through strong design and optimization. A multiobjective problem with BES deterioration and MG operational costs is used to construct the UC problem. A linear-weighted-sum method transforms the derived multiobjective problem into a single-objective model, and the impact of weight parameters on microgrid operational costs and BES lifetime is rigorously examined in this paper. It is also explored how the size of the BES affects the functioning of the MG. The PSO algorithm is the most widely used algorithm for complex real-time applications, and PSO proved to be a reliable tool for optimization problems with uncertainties and constraints. In addition, PSO is preferred in most industries compared to other metaheuristic algorithms. This motivated the authors to select PSO for this complex application. As discussed, the basic version of the PSO algorithm is applied to many real-world optimization problems, and it has proved its superiority in handling

unconstrained and constrained problems (Eberhart and Kennedy, 1995). However, PSO is trapped by local optima when applied to complex non-linear problems (Rezaee Jordehi, 2020c). Many PSO variants are introduced to solve complex optimization problems, and PSO with time-varying acceleration coefficients (TVAC) strategy is discussed and considered in this paper (Achayuthakan and Ongsakul, 2009; Sun et al., 2011; Ghasemi et al., 2019; Rezaee Jordehi and Jasni, 2013; Jordehi, 2016). The proposed algorithm is called as enhanced mixed PSO (EMPSO) algorithm and is recommended to solve mixed integer optimization problems, i.e., handle the continuous, integer, and binary decision variables. The binary version of the proposed EMPSO is obtained by employing different transfer functions (TFs), such as S-shaped (Manjula Devi et al., 2022), V-shaped (Agrawal et al., 2022), U-shaped (Ahmed et al., 2021), Tapper-shaped (He et al., 2022) etc., in the literature to transform the continuous algorithm to its binary version (Devi et al., 2022). This paper uses S-shaped, V-shaped, and Quadratic transfer functions to demonstrate each version's effectiveness. Out of many versions, the quadratic transfer function offers the best result for the proposed PSO algorithms (Manjula Devi et al., 2022; Jordehi, 2019). It has been shown that the TVAC framework promotes a good balance between cognitive and social aspects in the early phase and succeeding iterations. Based on the above-all discussions, the primary contributions and highlights of this study are given as follows.

- A new PSO variant called EMPSO is proposed to solve the mixed integer optimization problems, i.e., scheduling for UC in microgrid systems.
- The cognitive and social constants and inertial weight of EMPSO are modified using adaptive non-linear parameters.
- A part of the continuous decision variables of the UC problem is transformed using the quadratic transfer function.
- Uncertainties are considered in electricity price, load demand, and renewable power generation, and a multiobjective optimization model is also developed using a weighted-sum approach.
- Five case studies are considered to validate the proposed algorithm, and the performance of EMPSO is compared with other variants of PSO algorithm.

The remainder of this paper is structured as follows. Section 2 describes the problem formulation and mathematical modeling of the UC problem. Section 3 discusses the basic concepts of the PSO algorithm and also discusses the formulation procedure of the EMPSO algorithm. Section 4 comprehensively discusses the experimental investigations on various test scenarios and also presents the performance comparison of the proposed algorithm with different TFs. Section 5 concludes the paper with the future scope of the proposed approach.

2. Problem formulation

This section discusses the formulation of the objection function for the UC problem in the BES-integrated MG system. The UC optimization model is to lower the operational cost of the system by calculating the best scheduling and energy production for the existing generation units while meeting some constraints. The decision variables contain information about the condition of the BES and the power and status of dispatchable distributed generators (DDGs) at various points. The objective is described as a bi-objective optimization model, with the objectives being the MG operational costs and BES lifespan, respectively (Rezaee Jordehi, 2021b). In this paper, the timeframe of UC is taken to be 24 h with a resolution of 1 h. The condition of the BES device at a given time t is represented by v_t and it is found using Eq. (1).

$$v_t = \begin{cases} -1 \text{ for discharging} \\ +1 \text{ for charging} \\ 0 \text{ for idle} \end{cases} \tag{1}$$

Eq. (2) is used to compute the level of energy of the battery at a given time t.

$$E_t = \begin{cases} E_{t-1} + \eta_c P_c \text{ if } v_t = 1 \\ E_{t-1} - \left(\dfrac{P_d}{\eta_d}\right) \text{ if } v_t = -1 \\ E_{t-1} \text{ if } v_t = 0 \end{cases} \tag{2}$$

Eq. (3) can be used to determine the DoD of a battery at a given time t.

$$DoD_t = 1 - \left(\frac{E_t}{E_{max}}\right) \tag{3}$$

Eq. (4) can be used to calculate the maximum DoD that a battery can suffer during its operation surface.

$$DoD = \max(DoD_t) \tag{4}$$

Therefore, employing Table 1, we can determine the lifetime of BES, which is the primary objective in a multiobjective framework (J_1). In this paper, the Lead–acid BES device is considered for further analysis.

$$J_1 = \tau \tag{5}$$

Eq. (6) can be used to calculate the operational costs of dispatchable DGs. The operational cost can be expressed mathematically using a quadratic equation.

$$F_i^t = a_i + b_i \times P_i(t) + c_i \times \left(P_i(t)^2\right) \tag{6}$$

where $P_i(t)$ denotes the power of ith dispatchable distributed generator element at time t, and a_i, b_i, and c_i denote the coefficients of the ith dispatchable distributed generator element. The cost of MG functioning, which is the second objective, is computed by adding the sums of the four attributes listed below.

$$J_2 = \sum_{i=1}^{N}\sum_{t=1}^{24} F_i^t + \sum_{t=1}^{24} \rho_t P_{grid,t} + \sum_{i=1}^{N}\sum_{t=1}^{24} SD_{i,t} + \sum_{i=1}^{N}\sum_{t=1}^{24} SC_{i,t} \tag{7}$$

where ρ_t denotes the market pricing at time t, $P_{grid,t}$ represents the power exchange with the utility at time t, $SD_{i,t}$ denotes the shut-down cost of the ith dispatchable distributed generator element at time t, and $SC_{i,t}$ denotes the start-up cost of the ith dispatchable distributed generator element at time t. The value of $P_{grid,t}$ is negative if the power is exported to the utility and positive if the utility delivers the power. It is necessary to normalize the objective function values in relation to their respective values and make them comparable, and then they are summed up.

$$J_{1n} = \frac{J_1}{J_{1,base}} \tag{8}$$

$$J_{2n} = \frac{J_2}{J_{2,base}} \tag{9}$$

$$J = \omega_1 \times J_{1n} + \omega_2 \times J_{2n} \tag{10}$$

where ω_1 and ω_2 are weight factors to decompose the multiobjective optimization problem as a single-objective optimization problem. Eq. (11) should be properly maintained to sustain the

MG's real power balance.

$$D_t = \begin{cases} P_{grid,t} + \sum_{i=1}^{N}\sum_{t=1}^{24} P_{i,t} + \sum_{i=1}^{N_r}\sum_{t=1}^{24} P_{j,t} - P_c, & if \quad v_t = 1 \\ P_{grid,t} + \sum_{i=1}^{N}\sum_{t=1}^{24} P_{i,t} + \sum_{i=1}^{N_r}\sum_{t=1}^{24} P_{j,t}, & if \quad v_t = 0 \\ P_{grid,t} + \sum_{i=1}^{N}\sum_{t=1}^{24} P_{i,t} + \sum_{i=1}^{N_r}\sum_{t=1}^{24} P_{j,t} + P_c, & if \quad v_t = -1 \end{cases} \tag{11}$$

where $P_{j,t}$ denotes the power of a jth renewable distribution network at a given time t and N_r refers to the total number of renewable DGs accessible. As shown in Eq. (12), the output of each DG is restricted to a specific range within which it is permitted to operate.

$$u_{i,t}P_{i,l} \le P_{i,t} \le u_{i,t}P_{i,h} \tag{12}$$

where $u_{i,t}$ denotes the status of the ith DDG at time t and $P_{i,h}$ and $P_{i,l}$ denote the maximum and minimum power of the ith DDG at time t, correspondingly. Eq. (13) presents the ramp rate bounds of DGs.

$$\left.\begin{aligned} P_{i,t} - P_{i,t-1} &\le R_{u,i} \\ P_{i,t-1} - P_{i,t} &\le R_{d,i} \end{aligned}\right\} \tag{13}$$

where $R_{d,i}$ and $R_{u,i}$ denote ramp-down and ramp-up rates of the ith dispatchable DG. The start-up cost is the amount spent when a generating unit is powered on. Heating equipment must be warmed up before being used in a production environment. The procedure of warming up is costly, and as a result, it impacts the entire operational cost. A unit's restart cost is calculated by how long that has been out of commission. Various units have varying start-up costs, and the cost to bring unit i up to speed can be computed using Eq. (14).

$$SC_i{}^t = \left.\begin{aligned} SC_{i,hot} &\longrightarrow MDT_i \le T^t_{Off,i} \le MDT_i + T_{cold,i} \\ SC_{i,cold} &\longrightarrow T^t_{Off,i} > MDT_i + T_{cold,i} \end{aligned}\right\} \tag{14}$$

where $SC_{i,cold}$ and $SC_{i,hot}$ denote the cold and hot start-up cost of the ith thermal unit, respectively, MDT_i denotes minimum downtime of the ith thermal unit, $T^t_{Off,i}$ denotes the time duration that unit i was continuously off, and $T_{cold,i}$ denotes the time duration for cooling of unit i.

It is ensured by Eq. (15) that there is sufficient time for temperature variations to reduce after the shut-down or start-up of the DGs.

$$\left.\begin{aligned} ON_i &= T_{on,i}\left(u_{i,t} - u_{i,t-1}\right) \\ OFF_i &= T_{off,i}\left(u_{i,t-1} - u_{i,t}\right) \end{aligned}\right\} \tag{15}$$

where OFF_i and ON_i represent the successive OFF and ON times, respectively of the ith dispatchable DG unit, and $T_{off,i}$ and $T_{on,i}$ represent the minimum OFF and ON time of the ith dispatchable DG unit. To ensure that the link connecting MG and the utility does not exceed its power flow limitation, Eq. (16) must be satisfied.

$$-P_{grid,max} \le P_{grid,t} \le P_{grid,max} \tag{16}$$

where $P_{grid,max}$ represents the maximum power flow capability of the connection between the utility and the grid. The BES energy level (E_t) at any given time should be less than or equal to its ratings, and it has to be equal to or higher than a boundary, as shown in Eq. (17).

$$E_{min} \le E_t \le E_{max} \tag{17}$$

Table 1
Lifespan vs. DoDs for various BES types (Rezaee Jordehi, 2021b, 2020b).

DoD in %	Lifespan of different types of BES		
	NaS	NiCd	Lead-Acid
10	100 000	7900	8000
20	60 000	5800	2500
30	30 000	3400	1500
40	15 000	2000	950
50	10 000	1200	700
60	9000	900	590
70	7000	800	500
80	6000	700	450
90	5000	600	390
100	4000	500	350

3. Proposed enhanced mixed particle swarm optimizer (EMPSO) algorithm

When it comes to handling difficult, constrained, non-linear real-world optimization problems, metaheuristics are one of the most effective optimization algorithms. The metaheuristic algorithms are population-based and gradient-free approaches that attempt to explore a near-global result with less computational effort. They may handle an optimization problem and solve it in an iterative process. This section mainly discusses the basic version of PSO and the proposed EMPSO formulation.

3.1. Particle swarm optimizer (PSO) algorithm

The particle swarm optimizer (PSO) algorithm, developed in Eberhart and Kennedy (1995) and influenced by the social behavior of bird flocking, is an evolutionary algorithm capable of finding the optimal global solution. This algorithm performs by initially developing and dispersing a large random solution, called particles, throughout the N-dimensional search space during the first step of this process.

It is decided which positions are used from a specific time between two integers. The location of the ith particle is symbolized by a vector ($x_i = x_{1,i}, x_{2,i}, \ldots, x_{t,i}$). Following that, each particle is designated a fitness value based on its N -dimensional location, which is defined by the optimization problem, and every particle identifies the earlier best-explored position (p_{best}), as well as the best position that had the best fitness for the whole flock (g_{best}). The velocity (v) and position of each particle i (x_i) is presented in Eqs. (18) and (19), respectively.

$$v_i^{t+1} = v_i^t + C_1 \times rand_1 \times \left(P_{p,best} - x_i^t\right) + +C_2 \times rand_2 \times \left(P_{g,best} - x_i^t\right) \tag{18}$$

$$x_i^{t+1} = x_i^t + v_i^{t+1} \tag{19}$$

where t denotes the current iteration, $rand_1$ and $rand_2$ denote the random numbers between (0,1), $P_{p,best}$ and $P_{g,best}$ denote the personal best and global best position of the particle, and C_1 and C_2 denote the acceleration coefficients.

3.2. Improved particle swarm optimizer

It was discovered in Shi and Eberhart (1998) that the inertial weight could be included in the basic PSO, which considerably improved the characteristics of the existing PSO. The inertial weight (ω) is stated in Eqs. (20)–(21).

$$v_i^{t+1} = \omega \times v_i^t + C_1 \times rand_1 \times \left(P_{p,best} - x_i^t\right) + +C_2 \times rand_2 \times \left(P_{g,best} - x_i^t\right) \tag{20}$$

$$x_i^{t+1} = x_i^t + v_i^{t+1} \tag{21}$$

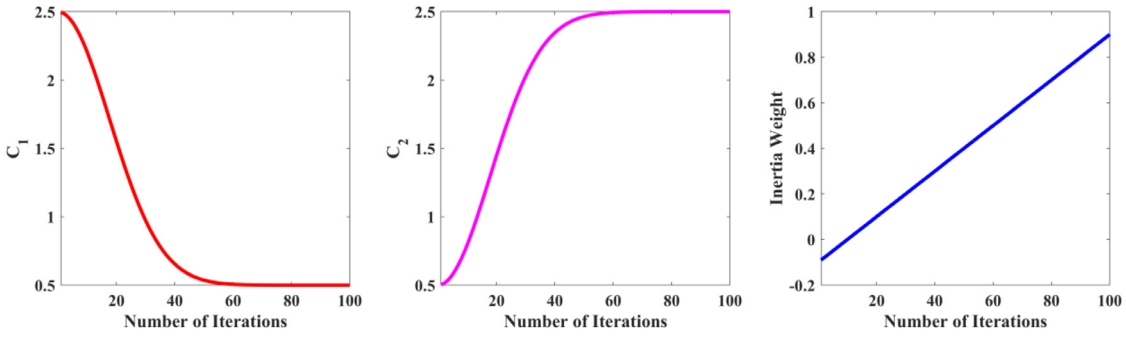

Fig. 1. Acceleration coefficients and inertia weight update over the number of iterations.

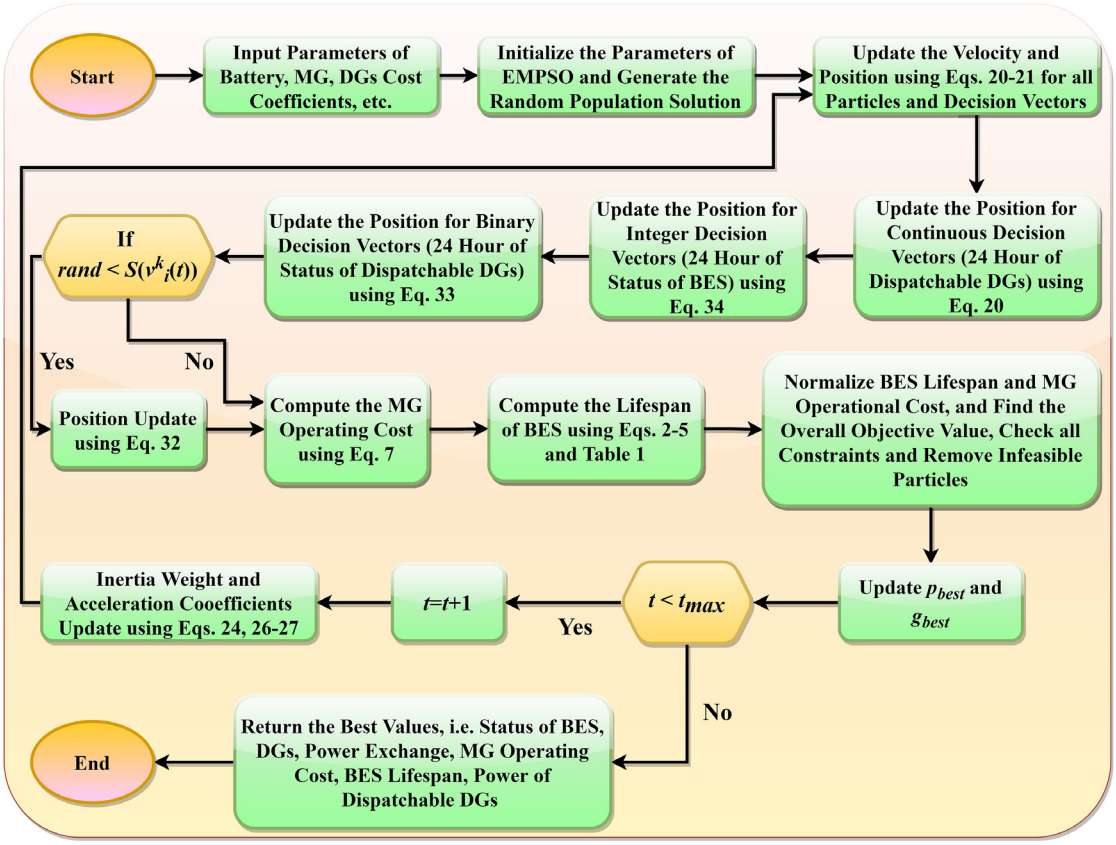

Fig. 2. Complete flow of proposed UC strategy for MG with energy storage.

There are several inertial weight schemes to choose from, each with its advantages and disadvantages. The following are different inertia weight factors to improve the performance of the PSO algorithm (Sun et al., 2011; Ghasemi et al., 2019; Rezaee Jordehi and Jasni, 2013).

$$\omega = \omega_{max} - (\omega_{max} - \omega_{min}) \times \frac{t}{t_{max}} \tag{22}$$

$$\omega = \omega - \frac{(\omega_{max} - \omega_{min})}{t_{max}} \tag{23}$$

$$\omega = (\omega_{max} - \omega_{min}) - \frac{(t_{max} - t)}{t_{max}} + \omega_{min} \tag{24}$$

$$\omega = \frac{2}{\left(\varphi - 2 + \sqrt{\varphi^2 - 4\varphi}\right)} + \omega_{damp};\ \varphi = \varphi_1 + \varphi_2 \tag{25}$$

where ω_{max} denotes maximum inertia weight, ω_{min} denotes minimum inertia weight, t_{max} denotes the maximum number of iterations, ω_{damp} denotes inertia weight damping ratio, and φ_1 and φ_2 denote the constriction coefficients (=2.05).

3.3. Proposed EMPSO algorithm

For this research, the authors have chosen a strategy expressed in Eq. (25), whose inertial weight reduces linearly with

Table 2
Various case studies.

Case Study (CS)	Details
CS1	UC in the absence of BES degradation and uncertainties
CS2	UC considering the uncertainties (load demand, market price, and renewable energy)
CS3	UC considering BES degradation
CS4	Effect on MG's operating cost due to different BES sizes
CS5	Effect on MG's operating cost due to different weight factors

Table 3
Various parameters of PSO and EMPSO.

Parameters	Value
Population size	20 000
t_{max}	100
ω_{min}	0.4
ω_{max}	0.9
C_{min}	0.5
C_{max}	2.2
Maximum velocity for continuous variables	0.1 times of decision variable range
Maximum velocity for binary variables	6

each iteration. In addition, a multivariate model of the PSO algorithm is used in this paper, wherein the acceleration coefficients are not constant. They adjust exponentially with each iterative process, resulting in better global search effectiveness and globally optimal convergence at the end of the exploration and faster global optimization convergence. With extensive testing in numerous applications, the proposed algorithm has proven superior to many other variations in localized exploitation and global explorations. The acceleration coefficients of the proposed algorithm are calculated using Eqs. (26) and (27).

$$C_1 = C_{min} + (C_{max} - C_{min}) \times \exp\left[-\left(\frac{4 \times t}{t_{max}}\right)^2\right] \tag{26}$$

$$C_2 = C_{max} - (C_{max} - C_{min}) \times \exp\left[-\left(\frac{4 \times t}{t_{max}}\right)^2\right] \tag{27}$$

where C_{min} and C_{max} denote the minimum and maximum value of acceleration coefficients. Fig. 1 illustrates the updates of acceleration coefficients and inertia weight over iterations.

The unit commitment in BES-integrated MGs is solved using an enhanced PSO variant considered in this research. When solving this challenge, three kinds of control variables/vectors are presented in this paper as follows: the output power of dispatchable DGs is a continuous vector/variable, the dispatchable DGs status is a binary variable/vector, and the status of the BES unit is an integer variable. Multiple approaches should be employed in order to cope with various types of control variables/vectors. Eq. (28) represents the position of the ith particle.

$$X_i = \left[X_{i,1}, X_{i,2}, \ldots, X_{i,dim}\right] \tag{28}$$

where *dim* denotes the problem dimensions. The particles are generated randomly, and the particle with the optimal objective is designated as the global optimum. For integer parameters, such as the condition of the BES part at various intervals, Eqs. (20) and (21) are executed on every iteration, and each parameter is normalized to the next integer value. Eqs. (20)–(21) are wholly irrelevant for binary variables in their original state. In binary PSO, for binary decision parameters, once the velocity vector has been modified with Eq. (20), an S-shaped transfer function and V-shaped transfer function and is defined by the following expressions are being used to map the velocity profile into the range [0,1] after the velocity vector have been updated with Eq. (20). Eq. (29) presents the sigmoidal (S-shaped) transfer function, which guides the particle i to travel in a binary position.

$$S\left(v_i^k(t)\right) = \frac{1}{1 + e^{-v_i^k(t)}} \tag{29}$$

where v_i^k represents the continuous velocity of particle i in dimension k at the current iteration t. Because the magnitude of the S-shaped transfer function appears to be continuous, it should be employed as a boundary for achieving the binary numbers. The S-shape transfer is a steady transformation function that turns an unbounded input into a bounded output. The fact that the transfer function's velocity is increasing improves the possibility of computing position vectors. The extensively employed stochastic threshold is utilized to ensure the binary value in a sigmoidal expression, as illustrated in Eq. (30), to achieve the binary value.

$$\overrightarrow{X\,(t+1)} = \begin{cases} 0, & \text{if } rand < S\left(v_i^k\,(t)\right) \\ 1, & \text{if } rand \geq S\left(v_i^k\,(t)\right) \end{cases} \tag{30}$$

where $v_i^k\,(t)$ and $\overrightarrow{X\,(t+1)}$ represent the velocity of the particle i in dimension k at each iteration t, and *rand* denotes the random number between (0,1). In addition to the S-shaped transfer function, this paper also uses the V-shaped transfer function to convert the decision variable into its binary form. The following expressions are useful to convert the part of the decision variable into its binary form.

$$S\left(v_i^k(t)\right) = \frac{2}{\pi} \times \operatorname{atan}\left(\frac{\pi}{2} \times v_i^k(t)\right) \tag{31}$$

$$\overrightarrow{X\,(t+1)} = \begin{cases} \overrightarrow{X\,(t)}^{-1}, & \text{if } rand < S\left(v_i^k(t)\right) \\ \overrightarrow{X\,(t)}, & \text{if } rand \geq S\left(v_i^k(t)\right) \end{cases} \tag{32}$$

where $\overrightarrow{X\,(t)}^{-1}$ denotes the complement of the binary decision variable $\overrightarrow{X\,(t)}$. The V-shaped transfer function benefits from not requiring the particle to acquire a value between 0 and 1 due to its shape. It permits the particle to turn to the compliments only when the fitness levels are high; otherwise, it would stay in the present location due to its lower fitness value.

Nevertheless, according to the study, the effectiveness of binary PSO, as represented by Eqs. (29)–(32) in addressing engineering optimization problems involving binary parameters is insufficient in these situations. This research presents an enhanced technique for handling binary classification variables, namely the state of dispatchable DGs decision variables. Eq. (20) is used to update the velocity in this strategy, and then Eq. (33) is used to map the updated velocities into the range [0,1] using a quadratic transfer function.

$$S\left(v_i^k\,(t)\right) = \begin{cases} \left(\dfrac{v_i^k\,(t)}{0.5 \times v_{max}}\right)^2, & \text{if } v_i^k\,(t) < 0.5 \times v_{max} \\ 1, & \text{if } v_i^k\,(t) \geq 0.5 \times v_{max} \end{cases} \tag{33}$$

where v_{max} denotes the maximum value of velocity. Particle locations are modified using Eq. (32) after the velocities associated with binary decision parameters have been mapped into the range [0,1]. The particle's position is updated for all integer decision vectors (24-hour status of BES units) using Eq. (34).

$$x_i^{t+1} = round\left(x_i^{t+1}\right) \tag{34}$$

The updated position x_i^{t+1} is obtained from Eq. (21) and rounded off to its integer values. Because the problem involves many uncertain input variables, which include 24-hour load demand, 24-hour production of renewable energy sources, and 24-hour market electricity price, because the uncertainties impact

both BES life span and MG operating cost, rigorous optimization is used to simulate the problem uncertainties. It is possible to create an uncertainty incorporated into the forecast error of data, and by utilizing a robust optimization algorithm, it is possible to obtain a robust decision variable over the uncertainty range. As depicted in Fig. 2, the proposed approach is organized. The Pseudocode of the proposed EMPSO algorithm is presented in the ***Algorithm***.

Algorithm: Pseudocode of Proposed EMPSO

Input : Initial parameters
Output : Optimal solutions

For *each particle* **do**
For *dim*=1:120 **do** % Continuous and Integer Decision vectors
Initialize particle using a random uniform distribution
End
For *dim*=121:216 **do** % Binary Decision vectors
If *rand*<0.5 **then** % *rand* is random number between [0,1]
Particle position = 0
Else
Particle position = 1
End If
End For
Initialize best position and velocity of the particle
End For
While stop condition is not met **do**
For each particle **do**
Evaluate objective function
Calculate particle velocity by Eq. 20
For *dim*=1:120 **do** % Continuous and Integer Decision vectors
Update the position using Eq. 20 (for continuous) and Eq. 34 (for Integer)
End For
For *dim*=121:216 **do** % Binary Decision vectors
Compute $S\left(v_i^k(t)\right)$ by Eq. 29 (S-shaped) or Eq. 31 (V-shaped) or Eq. 33 (Quadratic)
Update the position using Eq. 30 (for S-shaped) or Eq. 32 (for V-shaped and Quadratic)
End For
Calculate the fitness value
If *the fitness value* $\leq p_{best}$ **then**
Replace the current value by p_{best}
Calculate the g_{best}
End If
End For
Update the inertia weight and acceleration coefficients using Eq. 24 and Eq. 26-27.
End While
Return *Optimal solutions*

4. Results and discussions

This section describes how the proposed methodology has been used for unit commitment in BES-integrated grid-tied MGs and how the results are evaluated comprehensively. There are five different case studies used in the simulations. The details of the case studies are described in Table 2. All the five selected case studies are analyzed using the proposed EMPSO with an S-shaped transfer function named EMPSO-S, a V-shaped transfer function named EMPSO-V, and a quadratic transfer function named EMPSO-Q and a traditional PSO with a sigmoid transfer function named PSO-S. The algorithmic parameters of the PSO and the proposed EMPSO are listed in Table 3.

The considered MG in this study has four dispatchable DGs (microturbines) and two renewable DG sources with a maximum load demand of 16.14 MW at Hour 18 and minimum load demand of 8.47 MW at Hour 3. The required data for dispatchable DGs are listed in Table 4. The load demand, market electricity price, and the output of two renewable DGs (RDGs) are listed in Table 5. The demand and market price profiles are better illustrated in Fig. 3.

The maximum power transferred between MG and the utility is restricted to 10 MW. The dispatchable DGs (DDGs) is assumed to be turned off at the start. The MG's operating cost is $8971.2 if the battery energy storage unit is unused. The lead–acid battery is considered in this paper, and the battery storage unit specifications are provided in Table 6.

The uncertainty in renewable energy sources is 10%, the uncertainty in electricity market pricing is 3%, and the uncertainty in day-ahead forecasted load demand is 3% is considered in this paper to simulate the CS2.

4.1. Case study 1 (CS1)

This case study deals with the MG with BES integration. However, the battery degradation and uncertainties in demand, market price, and power ratings of RDGs are not considered. The rating of the battery storage system is considered to be 5 MW. The proposed algorithms, such as EMPSO-Q, EMPSO-V, and EMPSO-S, are functional to UC in microgrids with BES integration. In addition to the proposed algorithms, the conventional PSO-S is also applied to the same problem. The operating cost of the MG obtained for all the above-said algorithms is equal to $8729.87, $8962.13, $9935.88, and $12 536.3, respectively. To have a fair comparison, all the algorithms are executed ten times individually. Due to better performance, the optimal resource scheduling obtained by the EMPSO-Q is illustrated in Fig. 4. The status of the BES and depth of discharge (DoD) of the BES are illustrated in Fig. 5.

The absence of consideration for battery deterioration results in a maximum DoD of 94.5%, with a life span as limited as 350. MG operators can benefit from the BES unit by allowing it to recharge during a low-price period and discharge during a high-price period, allowing them to profit from energy exchange. Only when the profits generated by the pricing difference between two times greater than the cost of BES power losses is it acceptable to engage in power exchange between different periods. Table 7 shows the optimal state and power of generating units, as determined by the proposed EMPSO-Q.

From 1 h to 11 h, the market electricity price is lesser than the bid prices of DGs; therefore, the grid supplies the required demand. During 3 h, 5 h, and 9 h, the electricity price is less, i.e., 13.51 $/MWh, 18.51 $/MWh, and 21.84 $/MWh; therefore, the battery energy storage units get charged, and the amount payable is equal to $20.27, $27.77, and $32.76, respectively. The equal demand is calculated by subtracting the two renewable DGs power output and DDGs, and the grid must supply the equal demand. For instance, at 9 h, DG1 is ON, and it can supply up to 2.02 MW, and the BES unit charges to its maximum power, i.e., 1.5 MW, so the total available DDGs power is now available at 0.52 MW. At the same time, the equal demand is 10.52 MW at 9 h, which must be supplied by the grid (9.99 MW) and the DDG (0.52 MW). At 8 h, the battery is discharging due to the high market price. At this time, the revenue generation is $34.245. Despite the fact that the utility is the most cost-effective source, the utility cannot meet the entire demand of MG between 8 h to 10 h because the power flow restriction of the interconnection between the grid and MG is a binding limitation. As a result, DG1, the next most cost-effective resource, is initiated and supplied with a minimum power level of 2.02 MW. Fig. 6 illustrates the optimal status of all DGs during 24 h.

From 11 h onwards, DG1 is the most cost-effective power source; thus, it is supplied with the highest amount of energy.

Table 4
Data of all four dispatchable DGs (Rezaee Jordehi, 2021b).

DGs	a ($/MWh^2)	b ($/MWh)	c ($)	P_{min} (MW)	P_{max} (MW	Ramp-down and Ramp-up limit (MW/h)	T_{on} and T_{off} (H)	SC ($)	SD ($)
1	0	27.7	0	1	5	2.5	3	30	10
2	0	39.1	0	1	5	2.5	3	30	10
3	0	61.3	0	0.8	3	3	1	20	6
4	0	65.6	0	0.8	3	3	1	20	6

Table 5
Specifications of day-ahead load demand, market price, and power of RDGs (Rezaee Jordehi, 2021b).

Time	Load demand (MW)	Market price ($)	Output of RDG1 (MW)	Output of RDG2 (MW)	Time	Load demand (MW)	Market price ($)	Output of RDG1 (MW)	Output of RDG2 (MW)
1 h	8.73	15.03	0	0	13 h	13.92	65.79	0.40	0.81
2 h	8.54	10.97	0	0	14 h	15.27	66.57	0.37	1.20
3 h	8.47	13.51	0	0	15 h	15.36	65.44	0	1.23
4 h	9.03	15.36	0	0	16 h	15.69	79.79	0	1.28
5 h	8.79	18.51	0.63	0	17 h	16.13	115.45	0.05	1.00
6 h	8.81	21.80	0.80	0	18 h	16.14	110.28	0.04	0.78
7 h	10.12	17.30	0.62	0	19 h	15.56	96.05	0	0.71
8 h	10.93	22.83	0.71	0	20 h	15.51	90.53	0	0.92
9 h	11.19	21.84	0.68	0	21 h	14.00	77.38	0.57	0
10 h	11.78	27.09	0.35	0	22 h	13.03	70.95	0.6	0
11 h	12.08	37.06	0.62	0	23 h	9.82	59.42	0	0
12 h	12.13	68.95	0.36	0.75	24 h	9.45	56.68	0	0

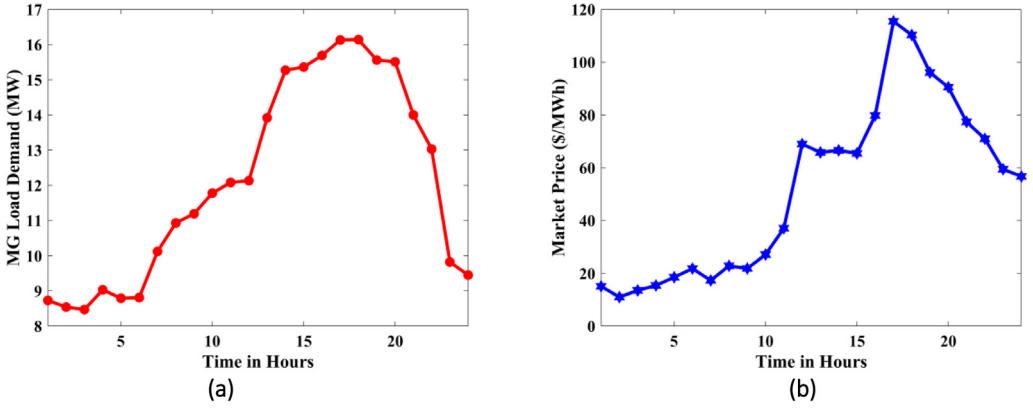

Fig. 3. Various profiles; (a) Demand profile, (b) Market price.

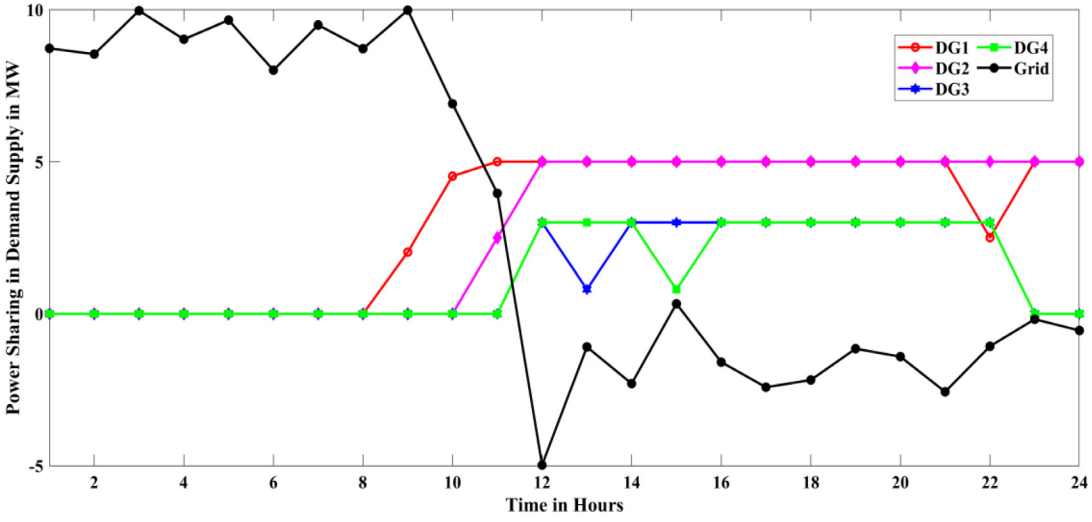

Fig. 4. Power-sharing of the DGs and grid in demand–supply for 24 h (CS1).

If required to function with maximum output and obtain the greatest possible profit from energy exchange at 11 h, DG1 must work with 4.52 MW at 11 h according to the ramp-up rate limit. During the 12 h to 22 h (except DG3 at 13 h, DG4 at 15 h, and DG1 at 22 h), all DGs, bidding available at a cheaper price, making it prudent to completely load them and export the

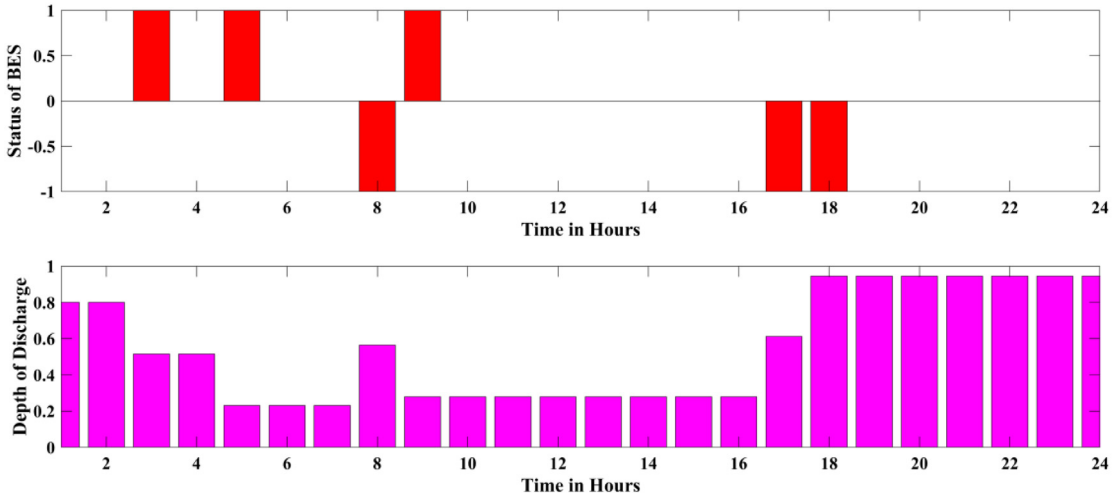

Fig. 5. Status of BES and DoD for 24 h (CS2).

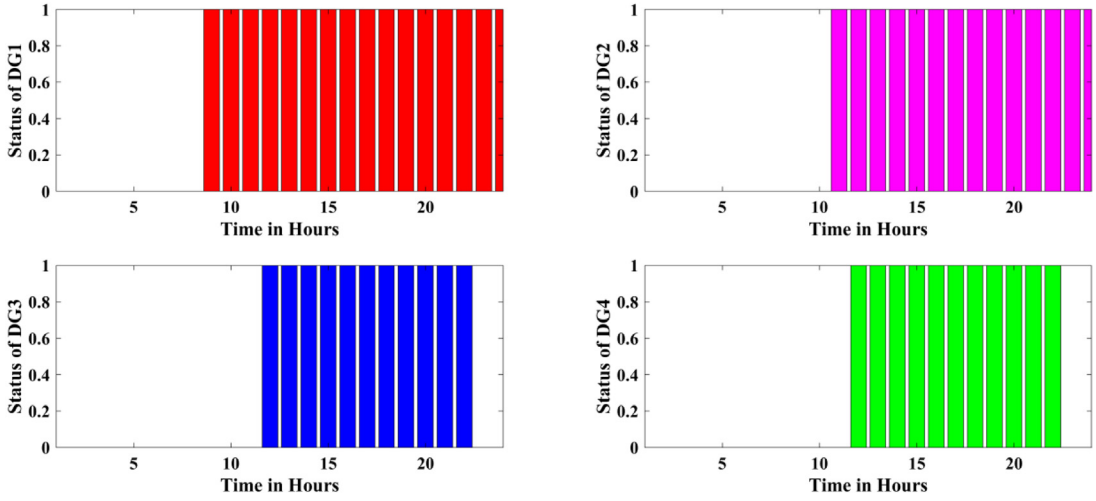

Fig. 6. Optimal Status of all DGs for 24 h by EMPSO-Q (CS1).

Table 6
Specification details of the BES unit.

Specifications	Values
Power rating (MW)	5 or 10
Charging and discharging powers (MW)	1.5
Minimum permissible energy level (MW)	0.2
Initial energy level (MW)	1
Charging efficiency (%)	95
Discharging efficiency (%)	90

excess energy to the utility, allowing you to get a huge income via energy exchange. BES is discharged at 17 h and 18 h, when the market price is pretty high, i.e., 115.45 $/MWh and 110.28 $/MWh, respectively, resulting in $173.18 and $165.42 in profit for MG. It is impossible to discharge BES after 19 h because the discharge causes it to exceed its maximum DoD limitation, as shown in Fig. 5. Because the market price is lowering from 20 h to 24 h, charging and discharging BES units at a reduced price is not a reasonable move. As a result, BES is idle for 20 h to 24 h. Due to the fact that the shut-down cost of DG3 and DG4 is much less than the losses incurred by operations with low power during 23 h and 24 h, these generators are turned off. For better understanding, Fig. 7 illustrates the dispatchable generation, power levels of DDGs, equal load demand, grid power, and the optimal BES status. For instance, at 17 h, the equal load demand of 15.08 MW is supplied by all DDGs (16 MW) and BES units (1.5 MW), and the remaining power, i.e., 2.42 MW, is supplied to the grid. Therefore, the revenue generation at 17 h is $(2.42*\$115.45) = \$279.389$.

4.2. Case study 2 (CS2)

Here, the uncertainties in load demand data, market pricing data, and renewable power for 24 h are considered, and robust optimization is employed to achieve the best possible results. The term "robust optimization" refers to a process in which an uncertainty range is constructed, and all proposed algorithms are applied to figure out a reliable solution throughout the entire uncertainty range. The forecast error for renewable energy production has been considered to be 10%, while the forecast error for load demand and the market price has been estimated to be 3%. The operating cost of the MG obtained by EMPSO-Q, EMPSO-V, EMPSO-S, and PSO-S equals $8986.98, $9869.55, $12 285.8, and $12 530.7. Due to better performance, the optimal resource scheduling obtained by the EMPSO-Q is illustrated in Fig. 8. The status of the BES unit and DoD of the BES is illustrated in Fig. 9.

Like CS1, the absence of consideration for battery deterioration results in a maximum DoD of 94.5%, with a life span as limited as

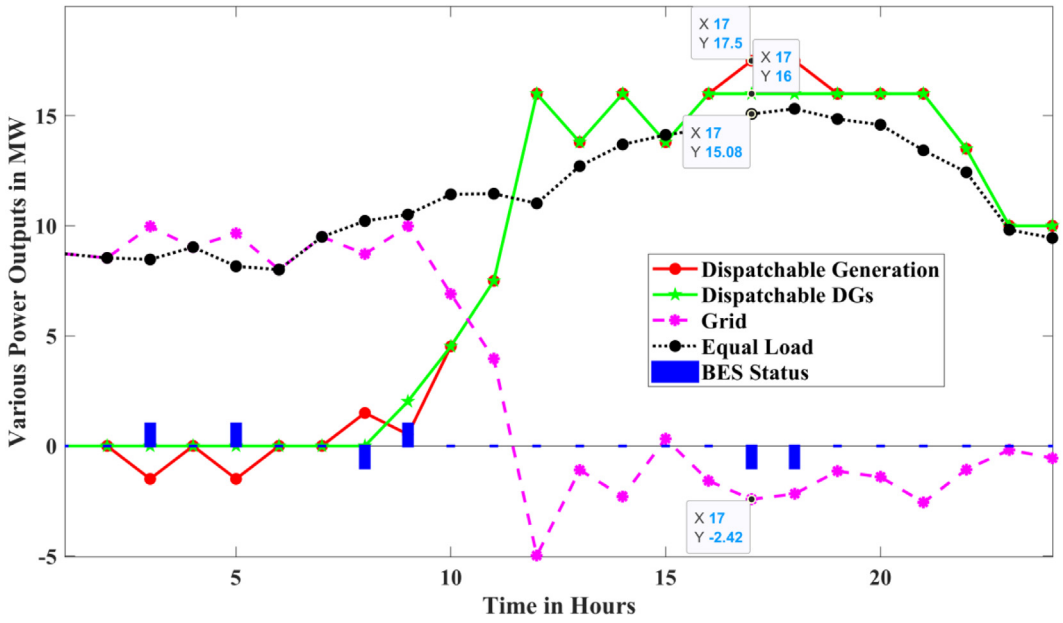

Fig. 7. Power-sharing of all DDGs, grid, and BES in demand–supply for 24 h (CS1).

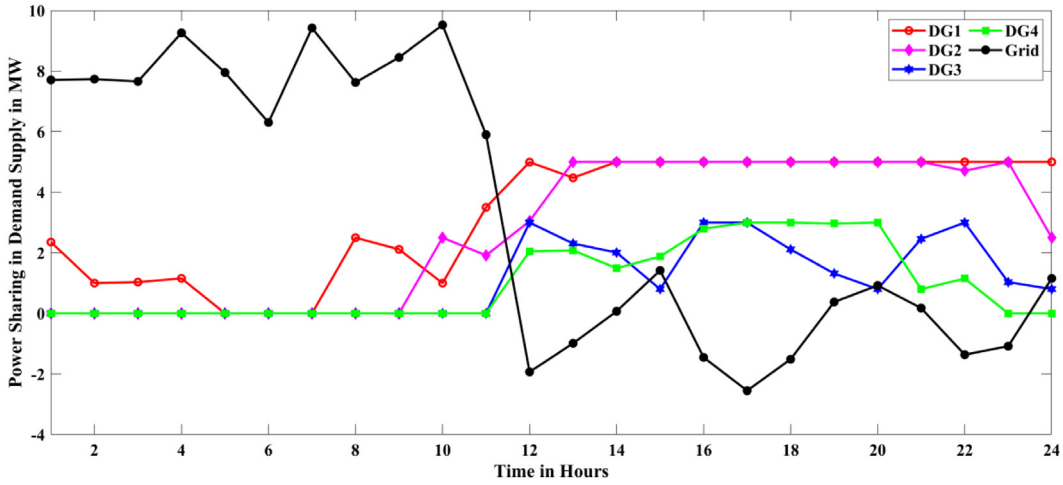

Fig. 8. Power-sharing of the DGs and grid in demand–supply for 24 h (CS2).

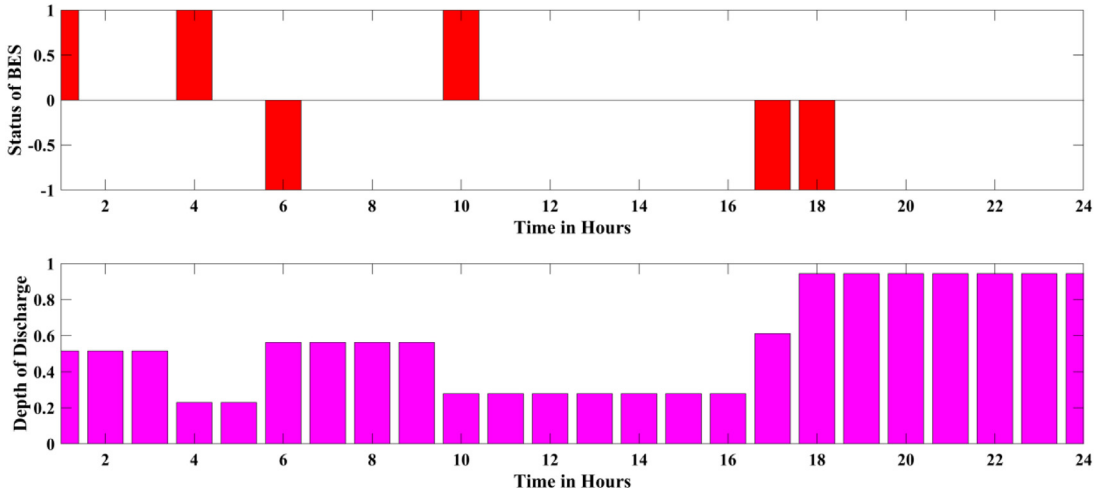

Fig. 9. Status of BES and DoD for 24 h (CS2).

Table 7
Optimal power and status of DGs with linear bid functions by EMPSO-Q (CS1).

Time	P1 (MW)	P2 (MW)	P3 (MW)	P4 (MW)	DDGs (MW)	Equal Demand (MW)	u1	u2	u3	u4	P_{grid} (MW)
1h	0.00	0.00	0.00	0.00	0.00	8.73	0	0	0	0	8.73
2h	0.00	0.00	0.00	0.00	0.00	8.54	0	0	0	0	8.54
3h	0.00	0.00	0.00	0.00	-1.50	8.47	0	0	0	0	9.97
4h	0.00	0.00	0.00	0.00	0.00	9.03	0	0	0	0	9.03
5h	0.00	0.00	0.00	0.00	-1.50	8.16	0	0	0	0	9.66
6h	0.00	0.00	0.00	0.00	0.00	8.01	0	0	0	0	8.01
7h	0.00	0.00	0.00	0.00	0.00	9.50	0	0	0	0	9.50
8h	0.00	0.00	0.00	0.00	1.50	10.22	0	0	0	0	8.72
9h	2.02	0.00	0.00	0.00	0.52	10.51	1	0	0	0	9.99
10h	4.52	0.00	0.00	0.00	4.52	11.43	1	0	0	0	6.91
11h	5.00	2.50	0.00	0.00	7.50	11.46	1	1	0	0	3.96
12h	5.00	5.00	3.00	3.00	16.00	11.02	1	1	1	1	-4.98
13h	5.00	5.00	0.80	3.00	13.80	12.71	1	1	1	1	-1.09
14h	5.00	5.00	3.00	3.00	16.00	13.70	1	1	1	1	-2.30
15h	5.00	5.00	3.00	0.80	13.80	14.13	1	1	1	1	0.33
16h	5.00	5.00	3.00	3.00	16.00	14.41	1	1	1	1	-1.59
17h	5.00	5.00	3.00	3.00	17.50	15.08	1	1	1	1	-2.42
18h	5.00	5.00	3.00	3.00	17.50	15.32	1	1	1	1	-2.18
19h	5.00	5.00	3.00	3.00	16.00	14.85	1	1	1	1	-1.15
20h	5.00	5.00	3.00	3.00	16.00	14.59	1	1	1	1	-1.41
21h	5.00	5.00	3.00	3.00	16.00	13.43	1	1	1	1	-2.57
22h	2.50	5.00	3.00	3.00	13.50	12.43	1	1	1	1	-1.07
23h	5.00	5.00	0.00	0.00	10.00	9.82	1	1	0	0	-0.18
24h	5.00	5.00	0.00	0.00	10.00	9.45	1	1	0	0	-0.55

350. MG operators can benefit from the BES unit by allowing the unit to recharge during a low-price period and discharge during a high-price period, allowing them to profit from energy exchange. Table 8 shows the optimal state and power of generating units obtained by the proposed EMPSO-Q. Compared to Table 7, the operating cost of the MG is significantly increased due to the consideration of uncertainties. Nevertheless, the obtained solution is robust in the face of uncertainties in renewable energy generation, load demand, and price; that is, no variance of uncertain data from the specified uncertainty set can result in an operating cost that is significantly greater than the attained operation cost, which is a significant improvement over previous solutions.

When analyzing the performance with scenario 1, it is clear that considering uncertainties has resulted in a $257.98 increase in the operating costs of MG. Although the result found in this case is resilient, the variations in market price, renewable energy, and load demand within the uncertainty range do not result in an operating cost greater than $8986.98, which is the maximum cost of operation. As previously stated, the ON/OFF condition and scheduling of MG sources are primarily influenced by changes in market pricing and equal demand, as well as other factors. In accordance with Figs. 8 and 9, the incorporation of uncertainties has impacted the optimal scheduling of resources, and in particular, the BES scheduling. It is important to note that BES is charged during less price durations of 1 h, 4 h, and 10 h and discharged during high price durations of 6 h, 17 h, and 18 h. The optimal status of all DGs for 24 h is illustrated in Fig. 10. Similar to CS1, Fig. 11 illustrates the dispatchable generation, power levels of DDGs, equal load demand, grid power, and the optimal BES status. For instance, at 17 h, the equal load demand of 14.9471 MW is supplied by all DDGs (16 MW) and BES units (1.5 MW), and the remaining power, i.e., 2.55294 MW, is supplied to the grid. Therefore, the revenue generation at 17 h is (2.55294∗$115.45) = $294.737.

4.3. Case study 3 (CS3)

The deterioration of BES is taken into consideration and is incorporated into the purpose of the unit commitment problem. The operating cost of the MG and BES lifespan is considered a multiobjective model. The multiobjective optimization problem is transformed into a single objective optimization problem using the linear weighted sum technique. The operation cost of the MG and BES unit life cycle is diverse; hence, they must be normalized before transforming into a single-objective problem. BES life span has been normalized in relation to 350, which would be the BES lifecycle in CS1. The operating cost of the MG has been normalized to $8971.2, which is the operation cost without a BES unit. The aggregate objective values obtained by EMPSO-Q, EMPSO-V, EMPSO-S, and PSO-S equal 0.9539, 1.10, 1.3126, and 1.325, respectively. The results were obtained using the weight factors of 0.9 and 0.1. Due to better performance, the optimal resource scheduling obtained by the EMPSO-Q is illustrated in Fig. 12. The status of the BES unit and DoD of the BES is illustrated in Fig. 13.

Table 9 shows the optimal state and power of generating units obtained by the proposed EMPSO-Q. The optimal status of all DGs is illustrated in Fig. 14. The operating cost obtained by the PSO-S, EMPSO-V, and EMPSO-S is equal to $1.5406E+04, $1.1479E+04, and $1.5182E+04, respectively. The BES life span is 590, 590, and 390, respectively, and normalized objective values are 1.716, 1.279, and 1.692 and 0.593, 0.593, and 0.897, respectively.

The operating cost, BES life span, normalized objective value, and normalized BES life span obtained by the proposed EMPSO-Q equals $8917.7, 590, 0.9941, and 0.593, respectively. In CS3, the BES life span improves from 350 to 590, while the operating cost of the MG increases from $8729.87 to $8917.7. When comparing UC outcomes between CS1 and CS3, it is clear that by considering BES deterioration in the fitness function, the BES life span rises

Table 8
Optimal power and status of DGs with linear bid functions by EMPSO-Q (CS2).

Time	P1 (MW)	P2 (MW)	P3 (MW)	P4 (MW)	DDGs (MW)	Equal Demand (MW)	u1	u2	u3	u4	P_{grid} (MW)
1h	2.35	0.00	0.00	0.00	0.85	8.56	1	0	0	0	7.71
2h	1.00	0.00	0.00	0.00	1.00	8.73	1	0	0	0	7.73
3h	1.03	0.00	0.00	0.00	1.03	8.69	1	0	0	0	7.66
4h	1.16	0.00	0.00	0.00	-0.34	8.92	1	0	0	0	9.26
5h	0.00	0.00	0.00	0.00	0.00	7.95	0	0	0	0	7.95
6h	0.00	0.00	0.00	0.00	1.50	7.80	0	0	0	0	6.30
7h	0.00	0.00	0.00	0.00	0.00	9.42	0	0	0	0	9.42
8h	2.50	0.00	0.00	0.00	2.50	10.12	1	0	0	0	7.62
9h	2.11	0.00	0.00	0.00	2.11	10.56	1	0	0	0	8.45
10h	1.00	2.50	0.00	0.00	2.00	11.52	1	1	0	0	9.52
11h	3.50	1.91	0.00	0.00	5.41	11.31	1	1	0	0	5.90
12h	4.99	3.04	3.00	2.05	13.08	11.15	1	1	1	1	-1.93
13h	4.48	5.00	2.31	2.08	13.86	12.87	1	1	1	1	-0.99
14h	5.00	5.00	2.01	1.49	13.50	13.56	1	1	1	1	0.07
15h	5.00	5.00	0.80	1.88	12.68	14.09	1	1	1	1	1.42
16h	5.00	5.00	3.00	2.80	15.80	14.34	1	1	1	1	-1.45
17h	5.00	5.00	3.00	3.00	17.50	14.95	1	1	1	1	-2.55
18h	5.00	5.00	2.11	3.00	16.61	15.10	1	1	1	1	-1.51
19h	5.00	5.00	1.32	2.97	14.29	14.66	1	1	1	1	0.37
20h	5.00	5.00	0.80	3.00	13.80	14.72	1	1	1	1	0.92
21h	5.00	5.00	2.46	0.80	13.26	13.43	1	1	1	1	0.17
22h	5.00	4.71	3.00	1.15	13.86	12.49	1	1	1	1	-1.36
23h	5.00	5.00	1.03	0.00	11.03	9.95	1	1	1	0	-1.08
24h	5.00	2.50	0.80	0.00	8.30	9.45	1	1	1	0	1.15

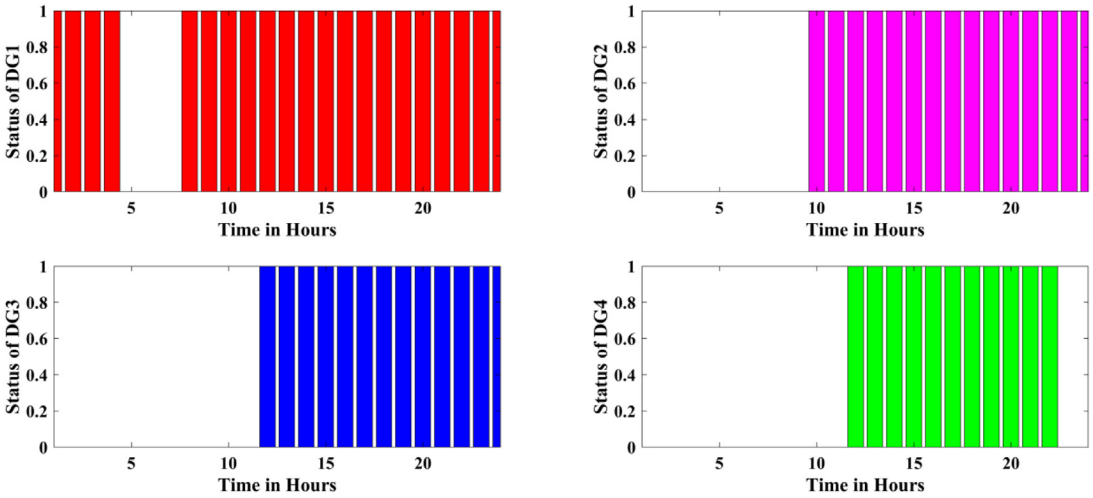

Fig. 10. Optimal Status of all DGs for 24 h by EMPSO-Q (CS2).

from 350 to 590. The BES unit is charged during 1 h and 3 h and discharged during 16 h.

Similar to CS1, Fig. 15 illustrates the dispatchable generation, power levels of DDGs, equal load demand, grid power, and the optimal BES status. For instance, at 16 h, the equal load demand of 14.41 MW is supplied by all DDGs (16 MW) and BES units (1.5 MW), and the remaining power, i.e., 3.09 MW, is supplied to the grid. Therefore, the revenue generation at 16 h is (3.09∗$79.79) = $246.551.

4.4. Case study 4 (CS4)

It is decided to utilize a 10 MW BES rather than the formerly used 5 MW BES to discover the influence of BES capacity on microgrid functioning. It is shown in Figs. 16 and 17 that the optimum scheduling of resources for UC could be achieved without considering uncertainty. The operation cost of the MG obtained by EMPSO-Q, EMPSO-V, EMPSO-S, and PSO-S equals $8453.33, $10 228, $12 079.1, and $12 588.8, respectively. Compared to CS1, the operating cost of MG is $276.54 lesser in CS4 due to the inclusion of the high capacity of the BES unit. Due to better performance, the optimal resource scheduling obtained by the EMPSO-Q is illustrated in Fig. 16. The status of the BES and DoD is illustrated in Fig. 17.

The absence of consideration for battery deterioration results in a maximum DoD of 90.25%, with a life span as limited as 350. MG operators can benefit from the BES unit by allowing the unit to recharge during a low-price period and discharge during a high-price period, allowing them to profit from energy exchange.

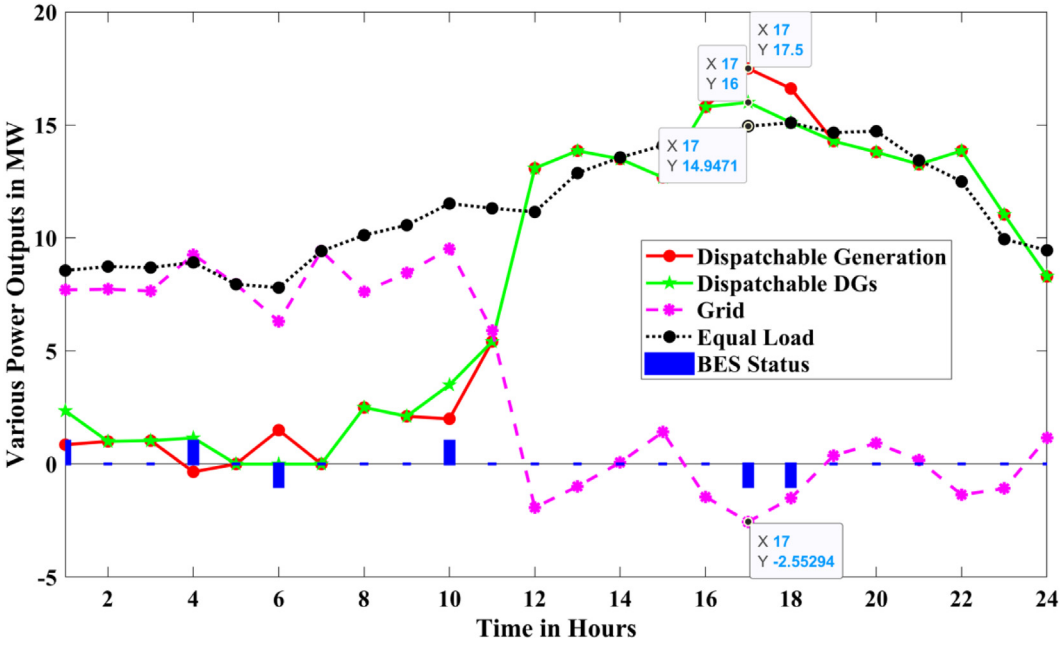

Fig. 11. Power-sharing of all DDGs, grid, and BES in demand–supply for 24 h (CS2).

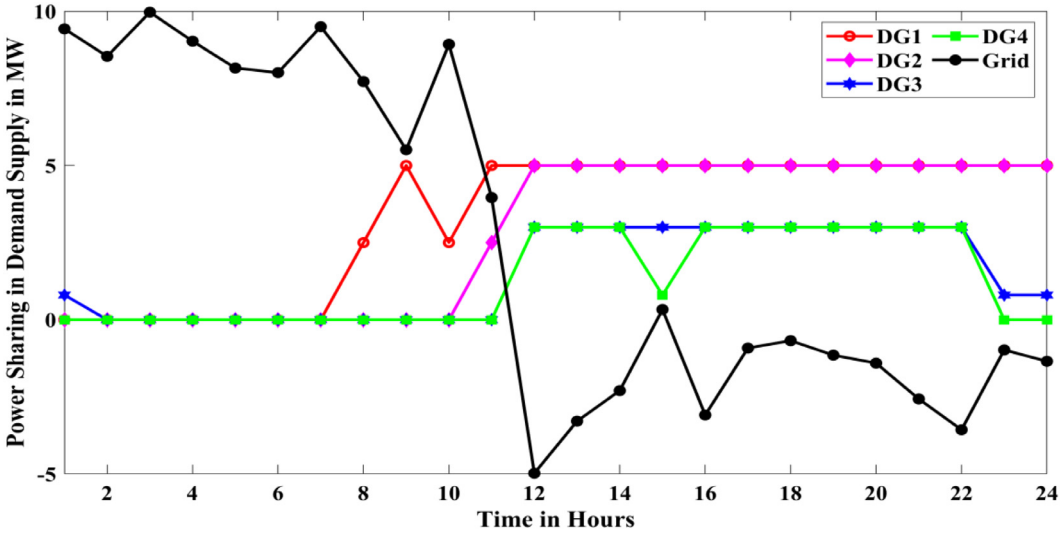

Fig. 12. Power-sharing of the DGs and grid in demand–supply for 24 h (CS3).

Table 10 shows the optimal state and power of generating units, as determined by the EMPSO-Q. The optimal status of all DGs is shown in Fig. 18.

Although due to its low energy potential, a 5 MW BES unit could only be charged for 3 h during the low-price hours 3 h, 5 h, and 9 h, a 10 MW BES can be charged for seven hours during the low-price hours 5 h, 6 h–10 h, and 15 h and be discharged over a longer period of time (14 h, 16 h–20 h), allowing the MG to participate in more energy arbitrage and lower its operating costs. Similar to CS1, Fig. 19 illustrates the dispatchable generation, power levels of DDGs, equal load demand, grid power, and the optimal BES status. For instance, at 18 h, the equal load demand of 15.32 MW is supplied by all DDGs (16 MW) and BES units (1.5 MW), and the remaining power, i.e., 2.18 MW, is supplied to the grid. Therefore, the revenue generation at 18 h is (2.18∗$110.28) = $240.411.

4.5. Case study 5 (CS5)

In CS5, unit commitment can be performed for diverse groups of weight factors in order to establish the impact of weight factors on the operating cost of MG and BES unit lifespan. A different pair of weight factors are considered, as listed in Table 11. Due to the better performance of EMPSO-Q in all earlier case studies, the operating cost of the MG, BES unit lifespan, and aggregate objective values obtained by the EMPSO-Q algorithm are listed. As discussed in CS4, where BES deterioration was disregarded, that is, where the weight factors for the operating cost of the MG and BES lifespan were 1 and 0, respectively, the operating cost of the

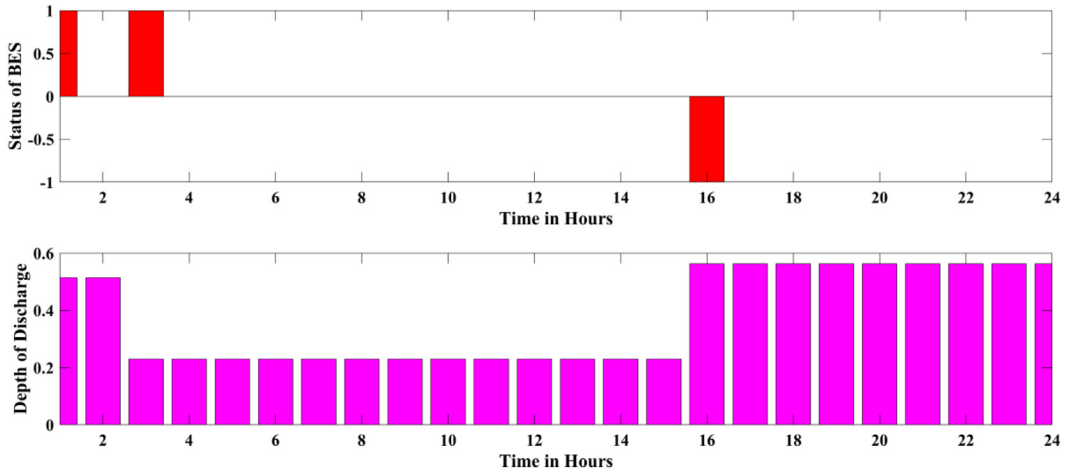

Fig. 13. Status of BES and DoD for 24 h (CS3).

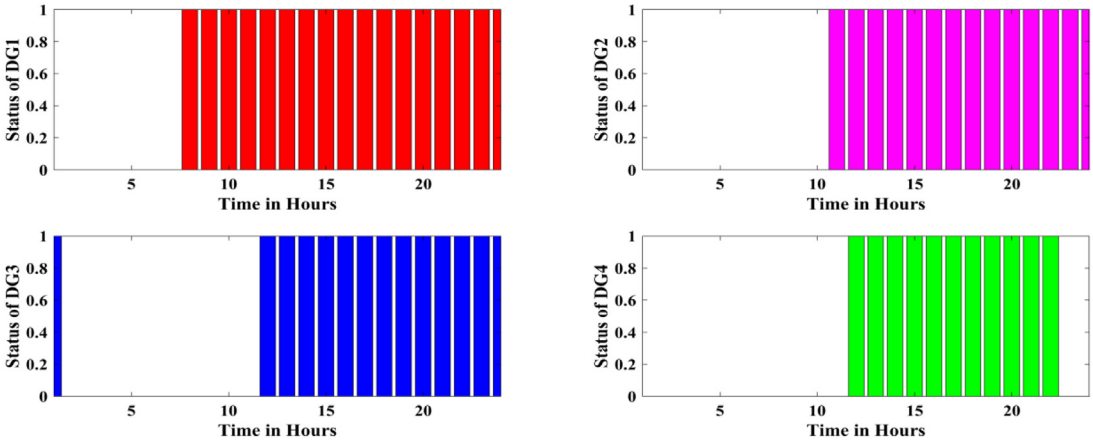

Fig. 14. Optimal Status of all DGs for 24 h by EMPSO-Q (CS3).

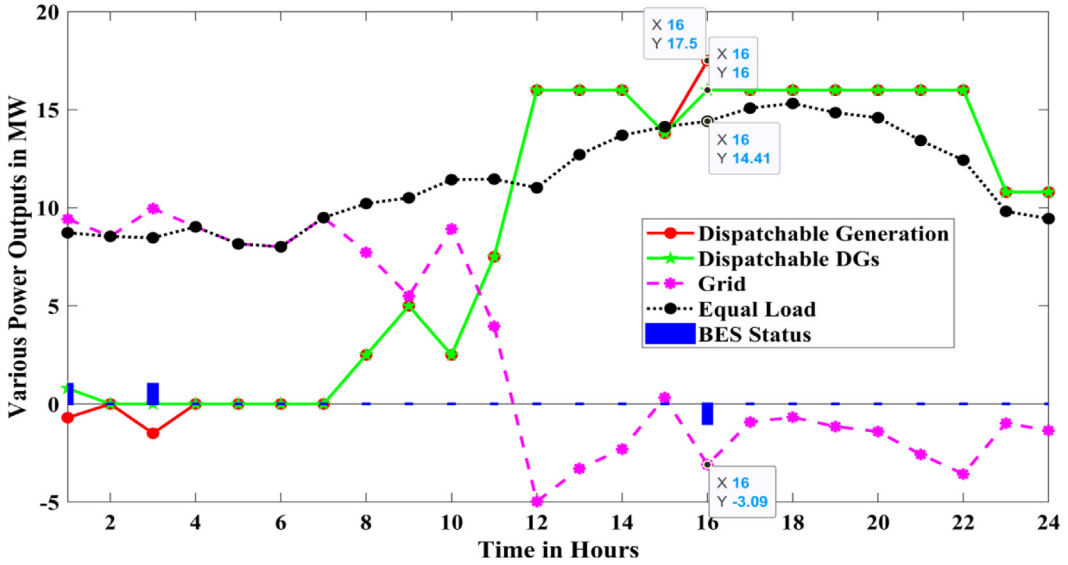

Fig. 15. Power-sharing of all DDGs, grid, and BES in demand–supply for 24 h (CS3).

Table 9
Optimal power and status of DGs with linear bid functions by EMPSO-Q (CS3).

Time	P1 (MW)	P2 (MW)	P3 (MW)	P4 (MW)	DDGs (MW)	Equal Demand (MW)	u1	u2	u3	u4	P_{grid} (MW)
1h	0.00	0.00	0.80	0.00	-0.70	8.73	0	0	1	0	9.43
2h	0.00	0.00	0.00	0.00	0.00	8.54	0	0	0	0	8.54
3h	0.00	0.00	0.00	0.00	-1.50	8.47	0	0	0	0	9.97
4h	0.00	0.00	0.00	0.00	0.00	9.03	0	0	0	0	9.03
5h	0.00	0.00	0.00	0.00	0.00	8.16	0	0	0	0	8.16
6h	0.00	0.00	0.00	0.00	0.00	8.01	0	0	0	0	8.01
7h	0.00	0.00	0.00	0.00	0.00	9.50	0	0	0	0	9.50
8h	2.50	0.00	0.00	0.00	2.50	10.22	1	0	0	0	7.72
9h	5.00	0.00	0.00	0.00	5.00	10.51	1	0	0	0	5.51
10h	2.50	0.00	0.00	0.00	2.50	11.43	1	0	0	0	8.93
11h	5.00	2.50	0.00	0.00	7.50	11.46	1	1	0	0	3.96
12h	5.00	5.00	3.00	3.00	16.00	11.02	1	1	1	1	-4.98
13h	5.00	5.00	3.00	3.00	16.00	12.71	1	1	1	1	-3.29
14h	5.00	5.00	3.00	3.00	16.00	13.70	1	1	1	1	-2.30
15h	5.00	5.00	3.00	0.80	13.80	14.13	1	1	1	1	0.33
16h	5.00	5.00	3.00	3.00	17.50	14.41	1	1	1	1	-3.09
17h	5.00	5.00	3.00	3.00	16.00	15.08	1	1	1	1	-0.92
18h	5.00	5.00	3.00	3.00	16.00	15.32	1	1	1	1	-0.68
19h	5.00	5.00	3.00	3.00	16.00	14.85	1	1	1	1	-1.15
20h	5.00	5.00	3.00	3.00	16.00	14.59	1	1	1	1	-1.41
21h	5.00	5.00	3.00	3.00	16.00	13.43	1	1	1	1	-2.57
22h	5.00	5.00	3.00	3.00	16.00	12.43	1	1	1	1	-3.57
23h	5.00	5.00	0.80	0.00	10.80	9.82	1	1	1	0	-0.98
24h	5.00	5.00	0.80	0.00	10.80	9.45	1	1	1	0	-1.35

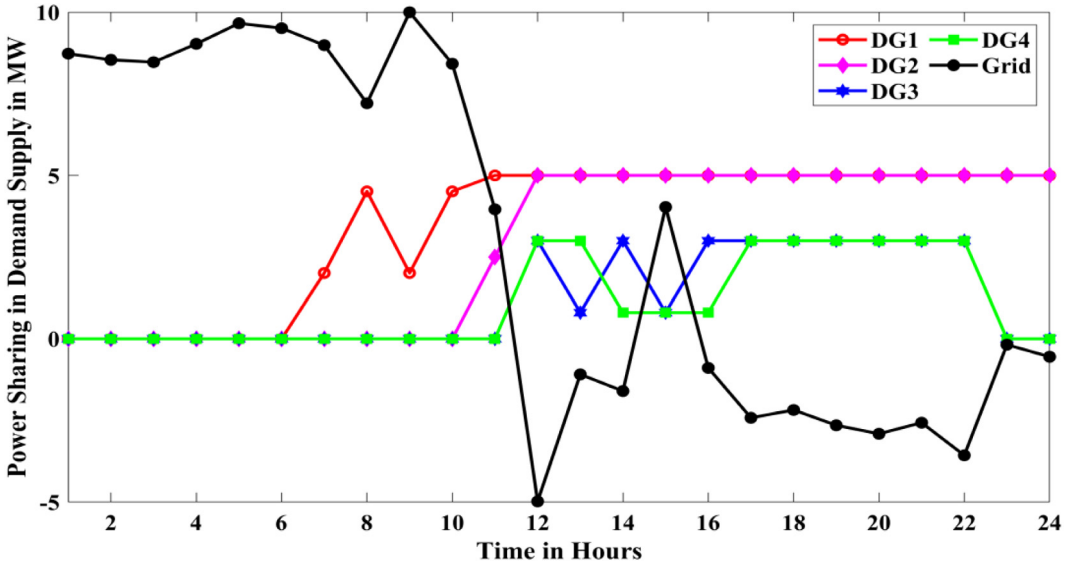

Fig. 16. Power-sharing of the DGs and grid in demand–supply for 24 h (CS4).

MG was $8999.11, and the BES lifespan was 350 (refer to CS1) with an aggregate objective value of 1.0031. When the weight factors for the MG and BES lifetime operating cost are modified to 0.8 and 0.2, respectively, the optimum schedule of microgrid resources is obtained. MG operation cost is $9.1055E+03, whereas BES lifespan is 590 for this set of weights, and the aggregate objective value is 0.9748. When the weight factors for the MG and BES lifetime operating cost are modified to 0.5 and 0.5, respectively, the optimal schedule of MG resources is obtained. MG operation cost is $9.1319E+03, whereas BES lifespan is 590 for this set of weights, and the combined objective value is 0.8067. When the weight factors for the MG and BES lifetime operating cost are modified to 0.2 and 0.8, respectively, the optimal schedule of MG resources is obtained. MG operation cost is $9.1506E+03, whereas BES lifespan is 590 for this set of weights, and the combined objective value is 0.6781. As predicted, the rise in the weight assigned to MG operation costs has resulted in an improvement in the operating cost of the MG and a decrease in the lifecycle of the BES. Due to better performance, the optimal resource scheduling obtained by the EMPSO-Q is illustrated in Fig. 20. The status of the BES unit and DoD of the BES is illustrated in Fig. 21.

For the weight factors of 0.8 and 0.2, the BES unit gets charged during 1 h and 2 h and discharged during 15 h. Table 12 shows the optimal state and power of generating units, as determined

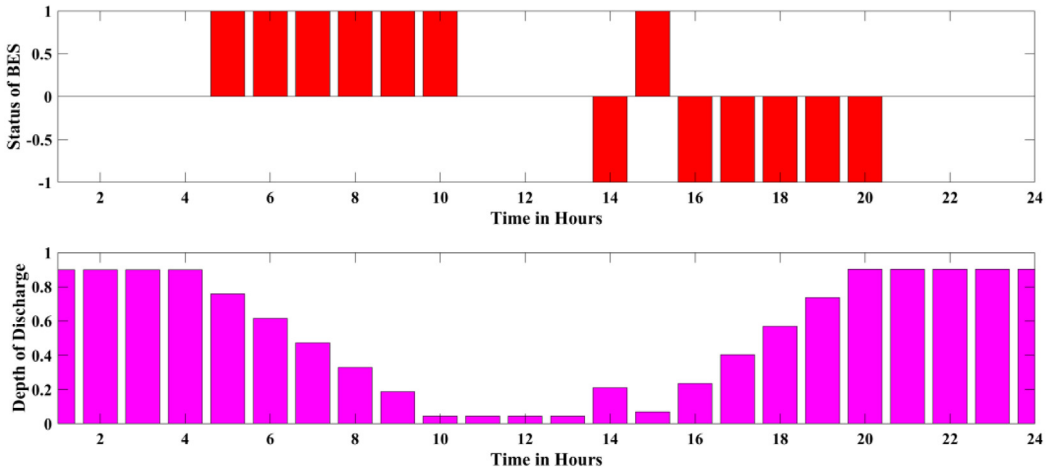

Fig. 17. Status of BES and DoD for 24 h (CS4).

Table 10
Optimal power and status of DGs with linear bid functions by EMPSO-Q (CS4).

Time	P1 (MW)	P2 (MW)	P3 (MW)	P4 (MW)	DDGs (MW)	Equal Demand (MW)	u1	u2	u3	u4	P_{grid} (MW)
1h	0.00	0.00	0.00	0.00	0.00	8.73	0	0	0	0	8.73
2h	0.00	0.00	0.00	0.00	0.00	8.54	0	0	0	0	8.54
3h	0.00	0.00	0.00	0.00	0.00	8.47	0	0	0	0	8.47
4h	0.00	0.00	0.00	0.00	0.00	9.03	0	0	0	0	9.03
5h	0.00	0.00	0.00	0.00	-1.50	8.16	0	0	0	0	9.66
6h	0.00	0.00	0.00	0.00	-1.50	8.01	0	0	0	0	9.51
7h	2.01	0.00	0.00	0.00	0.51	9.50	1	0	0	0	8.99
8h	4.51	0.00	0.00	0.00	3.01	10.22	1	0	0	0	7.21
9h	2.01	0.00	0.00	0.00	0.51	10.51	1	0	0	0	10.00
10h	4.51	0.00	0.00	0.00	3.01	11.43	1	0	0	0	8.42
11h	5.00	2.50	0.00	0.00	7.50	11.46	1	1	0	0	3.96
12h	5.00	5.00	3.00	3.00	16.00	11.02	1	1	1	1	-4.98
13h	5.00	5.00	0.80	3.00	13.80	12.71	1	1	1	1	-1.09
14h	5.00	5.00	3.00	0.80	15.30	13.70	1	1	1	1	-1.60
15h	5.00	5.00	0.80	0.80	10.10	14.13	1	1	1	1	4.03
16h	5.00	5.00	3.00	0.80	15.30	14.41	1	1	1	1	-0.89
17h	5.00	5.00	3.00	3.00	17.50	15.08	1	1	1	1	-2.42
18h	5.00	5.00	3.00	3.00	17.50	15.32	1	1	1	1	-2.18
19h	5.00	5.00	3.00	3.00	17.50	14.85	1	1	1	1	-2.65
20h	5.00	5.00	3.00	3.00	17.50	14.59	1	1	1	1	-2.91
21h	5.00	5.00	3.00	3.00	16.00	13.43	1	1	1	1	-2.57
22h	5.00	5.00	3.00	3.00	16.00	12.43	1	1	1	1	-3.57
23h	5.00	5.00	0.00	0.00	10.00	9.82	1	1	0	0	-0.18
24h	5.00	5.00	0.00	0.00	10.00	9.45	1	1	0	0	-0.55

by the proposed EMPSO-Q for the weight factors of 0.8 and 0.2. The optimal status of all DGs for the weight factors of 0.8 and 0.2 is illustrated in Fig. 22.

Similar to all case studies, Fig. 23 illustrates the dispatchable generation, power levels of DDGs, equal load demand, grid power, and the optimal BES status for the weight factors of 0.8 and 0.2. For instance, at 15 h, the equal load demand of 14.13 MW is supplied by all DDGs (16 MW) and BES units (1.5 MW), and the remaining power, i.e., 3.37 MW, is supplied to the grid. Therefore, the revenue generation at 18 h is (3.37∗$65.44) = $220.533.

4.6. Performance comparison and statistical analysis

In order to verify the performance of all selected algorithms, the statistical data, such as Min, Mean, standard deviation (STD), and runtime (RT), are listed and analyzed in this section. All selected algorithms are executed 10 times for each case study, and all the statistics parameters are listed in Table 13. Boldface letters in Table 13 indicate the best results. Also, in terms of the Min, Mean, and STD, EMPSO-Q outperforms the EMPSO-V, EMPSO-S, and PSO-S. Based on statistic parameters, EMPSO-Q stood first,

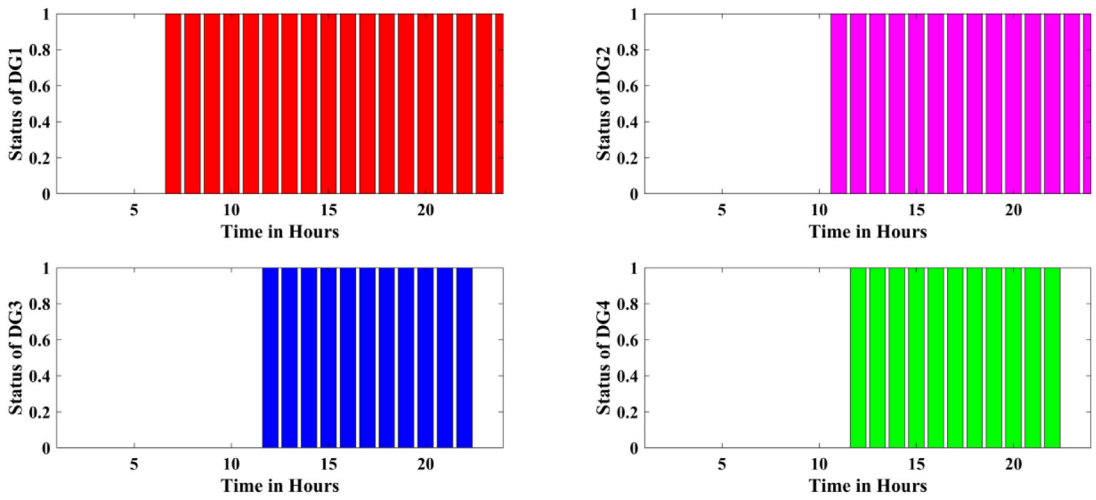

Fig. 18. Optimal Status of all DGs for 24 h by EMPSO-Q (CS4).

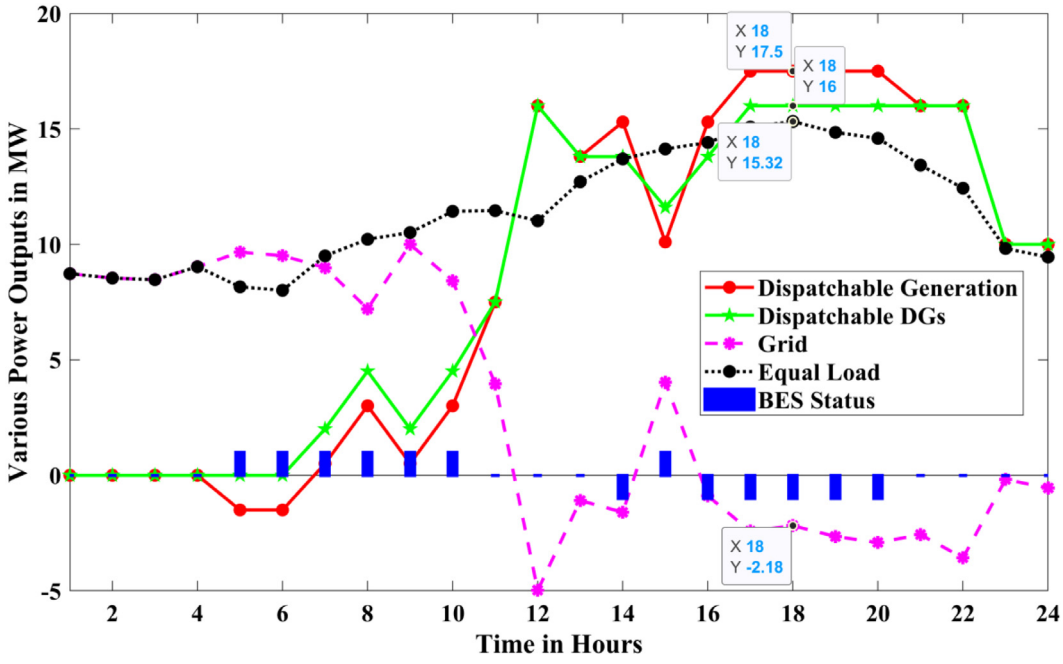

Fig. 19. Power-sharing of all DDGs, grid, and BES in demand–supply for 24 h (CS4).

Table 11
Various objective values for different weight factors.

Weight factors		MG cost ($)	BES Lifecycle	Aggregate objective values
ω_1	ω_2			
1	0	8.9991E+03	350	1.0031
0.8	0.2	9.1055E+03	590	0.9936
0.5	0.5	9.1319E+03	590	0.8067
0.2	0.8	9.1506E+03	590	0.6781

followed by EMPSO-V, EMPSO-S, and PSO-S. The RT value of PSO-S is less than all other selected algorithms for all case studies. However, the difference between the RT values obtained by PSO-S and EMPSO-Q is much less and almost negligible. Therefore, based on statistical data analysis, it was noticed that the proposed EMPSO-Q is a robust tool for the MG unit commitment problem.

To observe the convergence behavior of all algorithms, the convergence curve obtained by all algorithms in all case studies is illustrated in Fig. 24. From Fig. 24a–d, it was observed that the convergence behavior of EMPSO-Q is more excellent than all other selected algorithms. Due to the superior convergence performance of EMPSO-Q, the convergence curves obtained by EMPSO-Q for CS5 with different weights are illustrated for a better understanding of the weight factor's impact on operating cost and BES lifespan. The increase in the weight of operating costs has resulted in an improvement in operating costs and a decrease in the lifecycle of the BES.

Based on the obtained results and critical analysis, the proposed algorithm is considered to be a promising scheduling algorithm for the unit commitment problem of the microgrid systems considering the uncertainties. It has the benefits, such as simple implementation, quicker convergence, effective uncertainty handling, and low computational burden. Nevertheless, the proposed

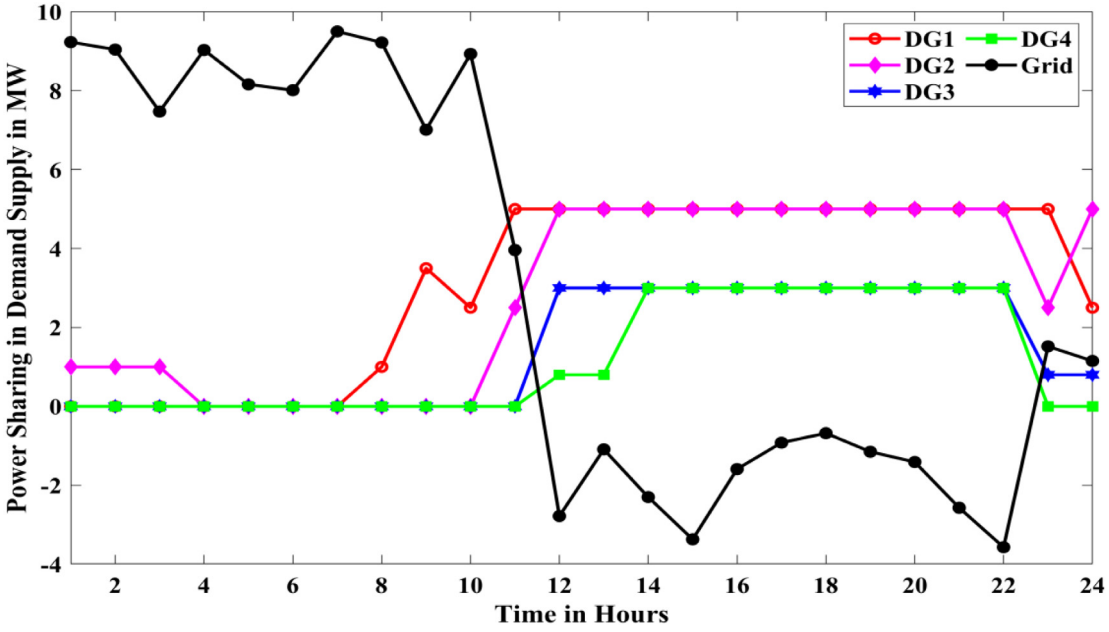

Fig. 20. Power-sharing of the DGs and grid in demand–supply for 24 h (weight factors of 0.8 and 0.2).

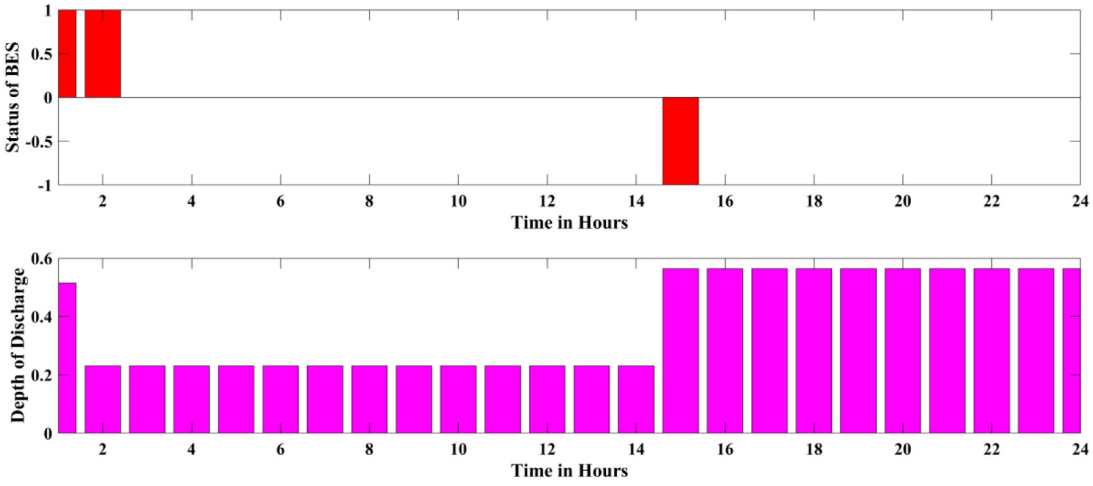

Fig. 21. Status of BES and DoD for 24 h (weight factors of 0.8 and 0.2).

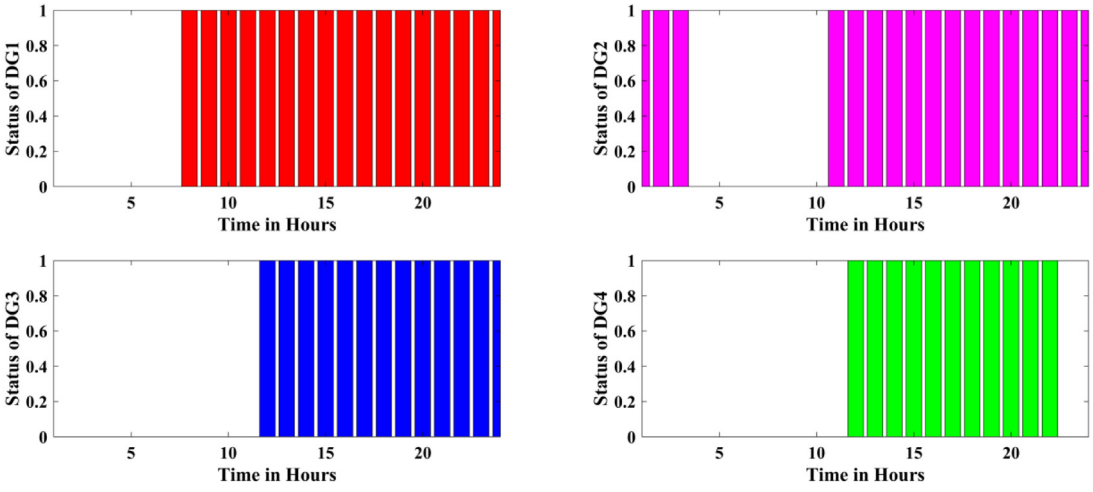

Fig. 22. Optimal Status of all DGs for 24 h by EMPSO-Q (weight factors of 0.8 and 0.2).

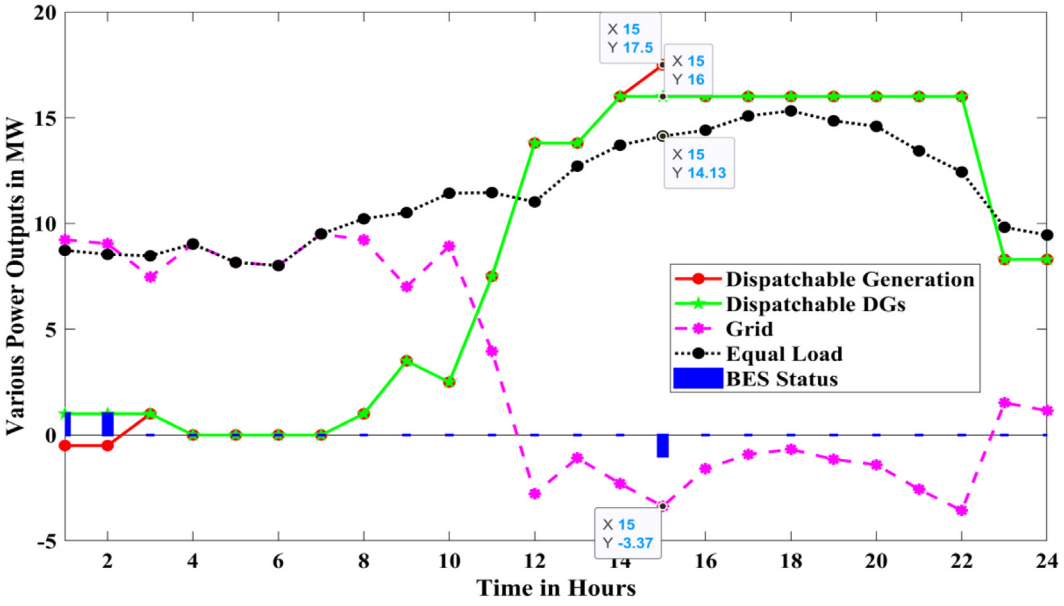

Fig. 23. Power-sharing of all DDGs, grid, and BES in demand–supply for 24 h (weight factors of 0.8 and 0.2).

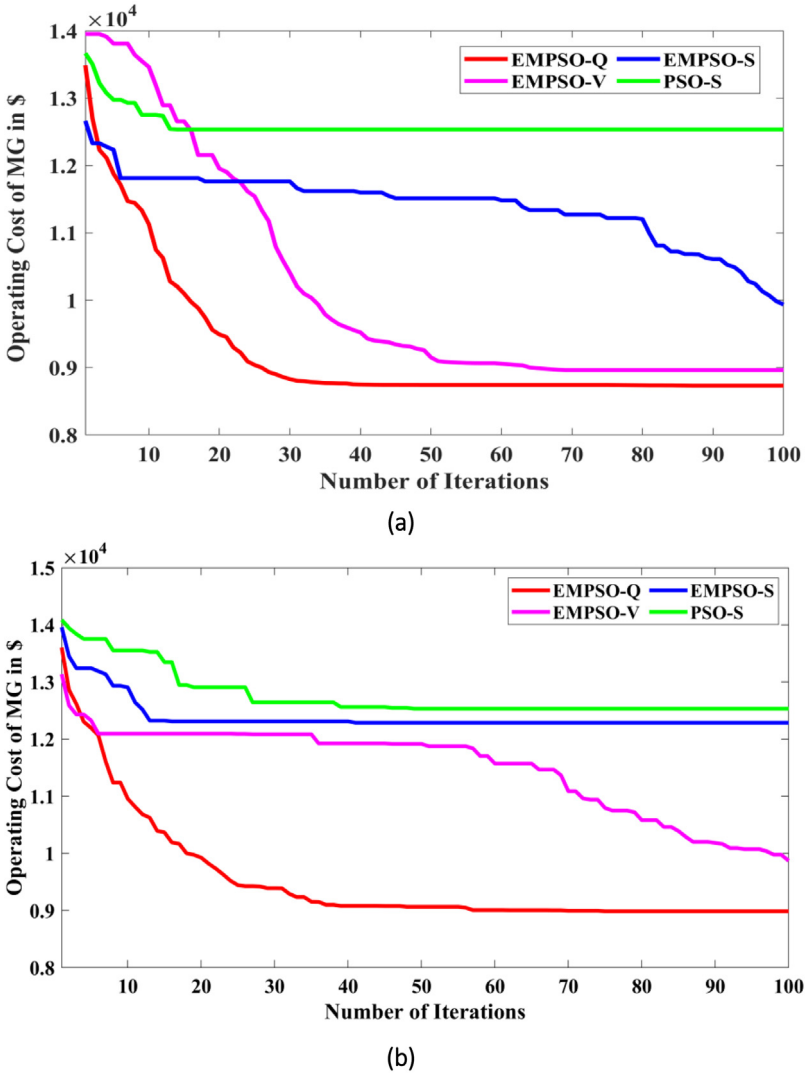

Fig. 24. Convergence curves; (a) CS1, (b) CS2, (c) CS3, (d) CS4, (e) CS5 with different weight factors.

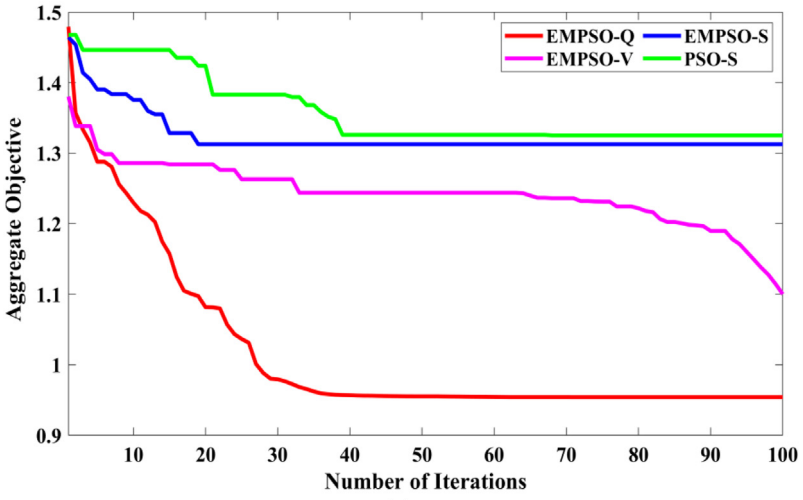

(c)

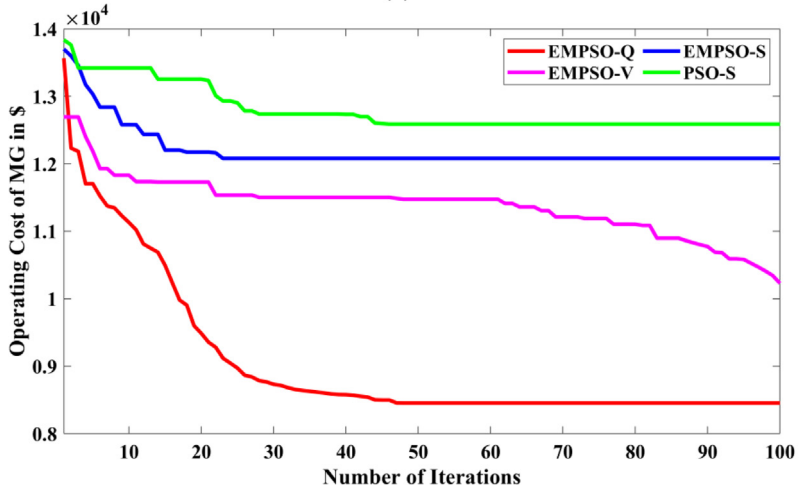

(d)

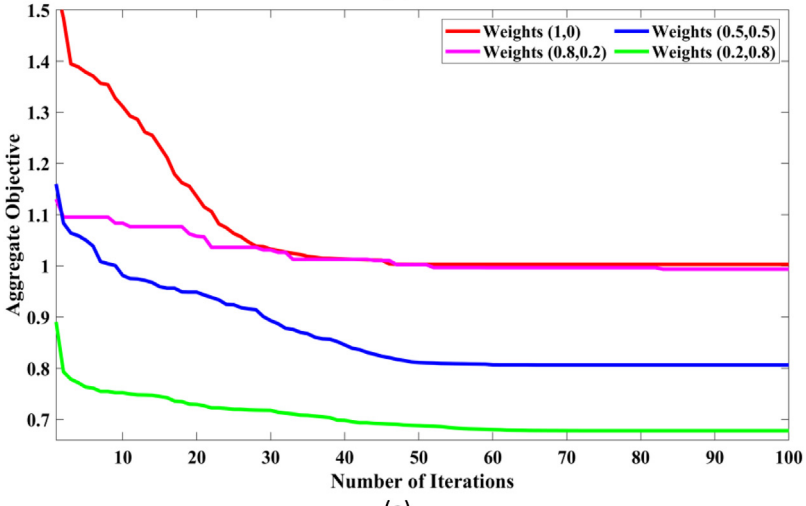

(e)

Fig. 24. (*continued*).

Table 12
Optimal power and status of DGs with linear bid functions by EMPSO-Q (CS5).

Time	P1 (MW)	P2 (MW)	P3 (MW)	P4 (MW)	DDGs (MW)	Equal Demand (MW)	u1	u2	u3	u4	P_{grid} (MW)
1h	0.00	1.00	0.00	0.00	-0.50	8.73	0	1	0	0	9.23
2h	0.00	1.00	0.00	0.00	-0.50	8.54	0	1	0	0	9.04
3h	0.00	1.00	0.00	0.00	1.00	8.47	0	1	0	0	7.47
4h	0.00	0.00	0.00	0.00	0.00	9.03	0	0	0	0	9.03
5h	0.00	0.00	0.00	0.00	0.00	8.16	0	0	0	0	8.16
6h	0.00	0.00	0.00	0.00	0.00	8.01	0	0	0	0	8.01
7h	0.00	0.00	0.00	0.00	0.00	9.50	0	0	0	0	9.50
8h	1.00	0.00	0.00	0.00	1.00	10.22	1	0	0	0	9.22
9h	3.50	0.00	0.00	0.00	3.50	10.51	1	0	0	0	7.01
10h	2.50	0.00	0.00	0.00	2.50	11.43	1	0	0	0	8.93
11h	5.00	2.50	0.00	0.00	7.50	11.46	1	1	0	0	3.96
12h	5.00	5.00	3.00	0.80	13.80	11.02	1	1	1	1	-2.78
13h	5.00	5.00	3.00	0.80	13.80	12.71	1	1	1	1	-1.09
14h	5.00	5.00	3.00	3.00	16.00	13.70	1	1	1	1	-2.30
15h	5.00	5.00	3.00	3.00	17.50	14.13	1	1	1	1	-3.37
16h	5.00	5.00	3.00	3.00	16.00	14.41	1	1	1	1	-1.59
17h	5.00	5.00	3.00	3.00	16.00	15.08	1	1	1	1	-0.92
18h	5.00	5.00	3.00	3.00	16.00	15.32	1	1	1	1	-0.68
19h	5.00	5.00	3.00	3.00	16.00	14.85	1	1	1	1	-1.15
20h	5.00	5.00	3.00	3.00	16.00	14.59	1	1	1	1	-1.41
21h	5.00	5.00	3.00	3.00	16.00	13.43	1	1	1	1	-2.57
22h	5.00	5.00	3.00	3.00	16.00	12.43	1	1	1	1	-3.57
23h	5.00	2.50	0.80	0.00	8.30	9.82	1	1	1	0	1.52
24h	2.50	5.00	0.80	0.00	8.30	9.45	1	1	1	0	1.15

Table 13
Statistical parameters of all selected algorithms on all case studies.

Case study	Algorithm	Min	Mean	STD	RT
CS1	**EMPSO-Q**	**8729.87**	**8901.36**	**78.56**	6.404e+03
	EMPSO-V	8962.13	9125.41	124.43	6.543e+03
	EMPSO-S	9935.88	10 203.25	235.81	5.916e+03
	PSO-S	12 536.3	12 987.63	269.16	**5.224e+03**
CS2	**EMPSO-Q**	**8986.98**	**9145.47**	**81.24**	1.149e+04
	EMPSO-V	9869.55	10145.62	132.49	1.137e+04
	EMPSO-S	12 285.8	12 597.18	149.44	1.131e+04
	PSO-S	12 530.7	12 998.75	204.83	**1.128e+04**
CS3	**EMPSO-Q**	**0.9539**	**0.9978**	**0.0269**	1.078e+04
	EMPSO-V	1.10	1.362	0.1564	1.107e+04
	EMPSO-S	1.313	1.504	0.2143	1.081e+04
	PSO-S	1.325	1.6693	0.2245	**1.051e+04**
CS4	**EMPSO-Q**	**8453.33**	**8556.44**	**69.47**	1.041e+04
	EMPSO-V	10 228	10 469.11	110.45	1.058e+04
	EMPSO-S	12 079.1	12 369.78	136.56	1.039e+04
	PSO-S	12 588.8	12 997.37	198.37	**1.031e+04**
CS5 (0.8 and 0.2 weight)	**EMPSO-Q**	**0.9936**	**1.001**	**0.012**	1.081e+04
	EMPSO-V	1.145	1.211	0.023	1.114e+04
	EMPSO-S	1.308	1.398	0.045	1.094e+04
	PSO-S	1.335	1.412	0.074	**1.056e+04**

algorithm also has possible limitations, such as high computation time than the traditional PSO, convergence slows down in the later search phase, and it may fall into the local solutions occasionally. However, the above-said limitations are overcome by employing efficient boosting techniques, such as adaptive parameters (Premkumar et al., 2021b), the Chao mechanism (Premkumar et al., 2021a), hybrid algorithms (Premkumar et al., 2021), etc., and the same has been considered as the future scope of this study.

5. Conclusion

In MGs, unit commitment is a constrained, mixed continuous, integer, and binary optimization problem with stochastic inputs such as electricity market price, renewable energy generation, and load demand. In this study, BES deterioration has been considered in the unit commitment model in grid-connected microgrids. A new variant of the PSO algorithm is employed with different transfer functions to optimize continuous, binary,

and integer decision variables to handle unit commitment problems for the microgrid. For five different case studies, UC has indeed been handled. UC has been stated as a robust optimization method, considering the unpredictability of electricity market pricing, renewable energy generation, and load demand. The obtained findings confirm the effectiveness of the suggested algorithms over the basic PSO version, as well as the noticeable difference of BES on the saving of operating costs of MG. The addition of BES has improved the energy exchange capabilities of the microgrid while simultaneously lowering its operating costs. When uncertainties are considered, the findings reveal operational costs fall from $8729.87 to $8986.98. As a consequence of considering BES deterioration, the BES lifespan improves from 350 to 590, and the operating cost of the MG increases from $8729.87 to $8917.7. Furthermore, the impact of weight factors in a multiobjective optimization problem on the cost of MG operation and the lifespan of a BES has been examined. The findings in various case studies confirm that the EMPSO-Q algorithm outperforms EMPSO-V, EMPSO-S, and PSO-S in terms of performance.

The interval number technique may be used in future research to model the uncertainty associated with charging and discharging electric vehicles. In addition, the proposed algorithms may concentrate on a detailed parametric study of the robustness of the computational efficiency of the model parameters that have been provided in the literature. It is suggested to apply the proposed algorithms in transaction settlement, groundwater management, frequency assignment, cyber–physical systems, plant location, etc. The formulation of a typical guiding principle for specifying required model parameters depending on the complexity of the problem may further improve the broad application of proposed algorithms by increasing their universal application. Additionally, the perspective on energy efficiency for UC in relation to electric vehicles and the uncertainty in multiple energy sources might be explored.

CRediT authorship contribution statement

M. Premkumar: Conceptualization, Data curation, Methodology, Investigation, Visualization, Resources, Software, Supervision, Validation, Writing – original draft. **R. Sowmya:** Conceptualization, Data curation, Methodology, Formal analysis, Software, Visualization, Writing – original draft. **C. Ramakrishnan:** Data curation, Visualization, Resources, Writing – review & editing. **Pradeep Jangir:** Data curation, Visualization, Formal analysis, Software, Validation, Writing – original draft. **Essam H. Houssein:** Conceptualization, Validation, Writing – review & editing. **Sanchari Deb:** Validation, Funding, Writing – review & editing. **Nallapaneni Manoj Kumar:** Conceptualization, Validation, Visualization, Writing – review & editing.

Declaration of competing interest

The authors declare that they have no known competing financial interests or personal relationships that could have appeared to influence the work reported in this paper.

Data availability

All data generated or analyzed during this study are included in this published article [and its supplementary information files]. The readers are encouraged and suggested to follow https://premkumarmanoharan.wixsite.com/mysite for more updates with regard to this study.

Acknowledgment and funding

This project has received funding from the European Union's Horizon 2020 research and innovation programme under the Marie Skłodowska-Curie grant agreement No 945380

References

Abdulgalil, M.A., Khalid, M., Alismail, F., 2019. Optimal sizing of battery energy storage for a grid-connected microgrid subjected to wind uncertainties. Energies 12 (12), 2412. http://dx.doi.org/10.3390/EN12122412.

Abujarad, S.Y., Mustafa, M.W., Jamian, J.J., 2017. Recent approaches of unit commitment in the presence of intermittent renewable energy resources: A review. Renew. Sustain. Energy Rev. 70, 215–223. http://dx.doi.org/10.1016/J.RSER.2016.11.246.

Achayuthakan, C., Ongsakul, W., 2009. TVAC-PSO based optimal reactive power dispatch for reactive power cost allocation under deregulated environment. In: 2009 IEEE Power and Energy Society General Meeting. PES '09, http://dx.doi.org/10.1109/PES.2009.5275294.

Aghdam, F.H., Kalantari, N.T., Mohammadi-Ivatloo, B., 2020. A chance-constrained energy management in multi-microgrid systems considering degradation cost of energy storage elements. J. Energy Storage 29, 101416. http://dx.doi.org/10.1016/J.EST.2020.101416.

Agrawal, P., Ganesh, T., Oliva, D., Mohamed, A.W., 2022. S-shaped and V-shaped gaining-sharing knowledge-based algorithm for feature selection. Appl. Intell. 52 (1), 81–112. http://dx.doi.org/10.1007/S10489-021-02233-5/TABLES/13.

Ahmadi, A., Venayagamoorthy, G.K., Sharma, R., 2015. Performance of a smart microgrid with battery energy storage system's size and state of charge. pp. 1–7. http://dx.doi.org/10.1109/CIASG.2014.7127250.

Ahmed, S., Ghosh, K.K., Mirjalili, S., Sarkar, R., 2021. AIEOU: Automata-based improved equilibrium optimizer with U-shaped transfer function for feature selection. Knowl.-Based Syst. 228, 107283. http://dx.doi.org/10.1016/J.KNOSYS.2021.107283.

Alsaidan, I., Khodaei, A., Gao, W., 2017. A comprehensive battery energy storage optimal sizing model for microgrid applications.

Alsaidan, I., Khodaei, A., Gao, W., 2018. A comprehensive battery energy storage optimal sizing model for microgrid applications. IEEE Trans. Power Syst. 33 (4), 3968–3980. http://dx.doi.org/10.1109/TPWRS.2017.2769639.

Alvarado-Barrios, L., Rodríguez del Nozal, Á., Boza Valerino, J., García Vera, I., Martínez-Ramos, J.L., 2020. Stochastic unit commitment in microgrids: Influence of the load forecasting error and the availability of energy storage. Renew. Energy 146, 2060–2069. http://dx.doi.org/10.1016/J.RENENE.2019.08.032.

Alvarado-Barrios, L., Rodríguez del Nozal, A., Tapia, A., Martínez-Ramos, J.L., Reina, D.G., 2019. An evolutionary computational approach for the problem of unit commitment and economic dispatch in microgrids under several operation modes. Energies 12 (11), 2143. http://dx.doi.org/10.3390/EN12112143.

Bao, X., Xu, X., Zhang, Y., Xiong, Y., Shang, C., 2021. Optimal sizing of battery energy storage system in a shipboard power system with considering energy management optimization. Discrete Dyn. Nat. Soc. 2021, http://dx.doi.org/10.1155/2021/9032206.

Chaudhary, G., Lamb, J.J., Burheim, O.S., Austbø, B., 2021. Review of energy storage and energy management system control strategies in microgrids. Energies 14 (16), 4929. http://dx.doi.org/10.3390/EN14164929.

Chen, Y., Liu, Y., 2021. Congestion management of microgrids with renewable energy resources and energy storage systems. Front. Energy Res. 9, 388. http://dx.doi.org/10.3389/FENRG.2021.708087/BIBTEX.

Choudhury, S., 2020. A comprehensive review on issues, investigations, control and protection trends, technical challenges and future directions for microgrid technology. Int. Trans. Electr. Energy Syst. 30 (9), e12446. http://dx.doi.org/10.1002/2050-7038.12446.

Deckmyn, C., van de Vyver, J., Vandoorn, T.L., Meersman, B., Desmet, J., Vandevelde, L., 2017. Day-ahead unit commitment model for microgrids. IET Gener. Transm. Distrib. 11 (1), 1–9. http://dx.doi.org/10.1049/IET-GTD.2016.0222.

Devi, R.M., Premkumar, M., Jangir, P., Elkotb, M.A., Elavarasan, R.M., Nisar, K.S., 2022. IRKO: An improved runge–kutta optimization algorithm for global optimization problems. Comput. Mater. Contin. 70 (3), 4803–4827. http://dx.doi.org/10.32604/CMC.2022.020847.

Eberhart, R., Kennedy, J., 1995. A new optimizer using particle swarm theory. In: MHS'95. Proceedings of the Sixth International Symposium on Micro Machine and Human Science. pp. 39–43. http://dx.doi.org/10.1109/MHS.1995.494215.

Faisal, M., Hannan, M.A., Ker, P.J., Hussain, A., bin Mansor, M., Blaabjerg, F., 2018. Review of energy storage system technologies in microgrid applications: Issues and challenges. IEEE Access 6, 35143–35164. http://dx.doi.org/10.1109/ACCESS.2018.2841407.

Ferinar, M., Masoud, A.G., 2018. Battery swap station participation in microgrid unit commitment. In: CIRED Workshop on Microgrids and Local Energy Communities. p. 1.

Gao, D.W., 2015. Energy Storage for Sustainable Microgrid. pp. 1–142. http://dx.doi.org/10.1016/C2014-0-04144-5.

Gaurav, S., Birla, C., Lamba, A., Umashankar, S., Ganesan, S., 2015. Energy management of PV – Battery based microgrid system. Proc. Technol. 21, 103–111. http://dx.doi.org/10.1016/J.PROTCY.2015.10.016.

Ghasemi, M., Akbari, E., Zand, M., Hadipour, M., Ghavidel, S., Li, L., 2019. An efficient modified HPSO-TVAC-based dynamic economic dispatch of generating units. Electr. Power Compon. Syst. 47 (19–20), 1826–1840. http://dx.doi.org/10.1080/15325008.2020.1731876.

Gilani, M.A., Kazemi, A., Ghasemi, M., 2020. Distribution system resilience enhancement by microgrid formation considering distributed energy resources. Energy 191, 116442. http://dx.doi.org/10.1016/J.ENERGY.2019.116442.

He, Y., Zhang, F., Mirjalili, S., Zhang, T., 2022. Novel binary differential evolution algorithm based on Taper-shaped transfer functions for binary optimization problems. Swarm Evol. Comput. 69, 101022. http://dx.doi.org/10.1016/J.SWEVO.2021.101022.

Hittinger, E., Wiley, T., Kluza, J., Whitacre, J., 2015. Evaluating the value of batteries in microgrid electricity systems using an improved Energy Systems Model. Energy Convers. Manage. 89, 458–472. http://dx.doi.org/10.1016/J.ENCONMAN.2014.10.011.

Hong, Y.Y., Apolinario, G.F.D., Lu, T.K., Chu, C.C., 2022. Chance-constrained unit commitment with energy storage systems in electric power systems. Energy Rep. 8, 1067–1090. http://dx.doi.org/10.1016/J.EGYR.2021.12.035.

Huang, Z., Yang, F., 2021. Quality classification of lithium battery in microgrid networks based on smooth localized complex exponential model. Complexity 2021, http://dx.doi.org/10.1155/2021/6618708.

Invernizzi, G., Vielmini, G., 2018. Challenges in microgrid control systems design. An application case. In: 2018 110th AEIT International Annual Conference, AEIT 2018. http://dx.doi.org/10.23919/AEIT.2018.8577312.

Jadhav, A.M., Patne, N.R., Guerrero, J.M., 2019. A novel approach to neighborhood fair energy trading in a distribution network of multiple microgrid clusters. IEEE Trans. Ind. Electron. 66 (2), 1520–1531. http://dx.doi.org/10.1109/TIE.2018.2815945.

Jangir, P., Kumar, A., Rajasthan, R., 2017. A novel quasi opposition based passing vehicle search algorithm approach for large scale unit commitment problem. Glob. J. Res. Eng. 17, Accessed: Jan. 05, 2022. [Online]. Available: https://engineeringresearch.org/index.php/GJRE/article/view/1645.

Jiao, Y., Wu, J., Tan, Q.K., Tan, Z.F., Wang, G., 2017. An optimization model and modified harmony search algorithm for microgrid planning with ESS. Discrete Dyn. Nat. Soc. 2017, http://dx.doi.org/10.1155/2017/8425458.

Jordehi, A.R., 2016. Time varying acceleration coefficients particle swarm optimisation (TVACPSO): A new optimisation algorithm for estimating parameters of PV cells and modules. Energy Convers. Manage. 129, 262–274. http://dx.doi.org/10.1016/J.ENCONMAN.2016.09.085.

Jordehi, A.R., 2019. Binary particle swarm optimisation with quadratic transfer function: A new binary optimisation algorithm for optimal scheduling of appliances in smart homes. Appl. Soft Comput. 78, 465–480. http://dx.doi.org/10.1016/J.ASOC.2019.03.002.

Khalid, M., Ahmad, F., Panigrahi, B.K., Rahman, H., 2021. A capacity efficient power distribution network supported by battery swapping station. Int. J. Energy Res. http://dx.doi.org/10.1002/ER.7482.

Khorramdel, H., Aghaei, J., Khorramdel, B., Siano, P., 2016. Optimal battery sizing in microgrids using probabilistic unit commitment. IEEE Trans. Ind. Inform. 12 (2), 834–843. http://dx.doi.org/10.1109/TII.2015.2509424.

Kim, T.H., Shin, H., Kwag, K., Kim, W., 2020. A parallel multi-period optimal scheduling algorithm in microgrids with energy storage systems using decomposed inter-temporal constraints. Energy 202, 117669. http://dx.doi.org/10.1016/J.ENERGY.2020.117669.

Kumar, S., 2021. Cost-based unit commitment in a stand-alone hybrid microgrid with demand response flexibility. J. Inst. Eng. (India): Ser. B 2021, 1–11. http://dx.doi.org/10.1007/S40031-021-00634-1.

Lacap, J., Park, J.W., Beslow, L., 2021. Development and demonstration of microgrid system utilizing second-life electric vehicle batteries. J. Energy Storage 41, 102837. http://dx.doi.org/10.1016/J.EST.2021.102837.

Li, J., Zhou, S., Xu, Y., Zhu, M., Ye, L., 2021. A multi-band uncertainty set robust method for unit commitment with wind power generation. Int. J. Electr. Power Energy Syst. 131, 107125. http://dx.doi.org/10.1016/J.IJEPES.2021.107125.

Lijun, Z., Qingsheng, L., Guanhua, D., 2021. Planning and scheduling process for a grid-connected microgrid based on renewable energy sources by a novel fuzzy method. Complexity 2021, 1–16. http://dx.doi.org/10.1155/2021/8824278.

Mahmoud, M.S., 2017. Microgrid control problems and related issues. In: Microgrid: Advanced Control Methods and Renewable Energy System Integration. pp. 1–42. http://dx.doi.org/10.1016/B978-0-08-101753-1.00001-2.

Manjula Devi, R., Premkumar, M., Jangir, P., Santhosh Kumar, B., Alrowaili, D., Sooppy Nisar, K., 2022. BHGSO: Binary hunger games search optimization algorithm for feature selection problem. Comput. Mater. Contin. 70 (1), 557–579. http://dx.doi.org/10.32604/CMC.2022.019611.

Marzband, M., Alavi, H., Ghazimirsaeid, S.S., Uppal, H., Fernando, T., 2017. Optimal energy management system based on stochastic approach for a home microgrid with integrated responsive load demand and energy storage. Sustain. Cities Soc. 28, 256–264. http://dx.doi.org/10.1016/J.SCS.2016.09.017.

Mohammadi, S., Mohammadi, A., 2014. Stochastic scenario-based model and investigating size of battery energy storage and thermal energy storage for micro-grid. Int. J. Electr. Power Energy Syst. 61, 531–546. http://dx.doi.org/10.1016/J.IJEPES.2014.03.041.

Moncecchi, M., Brivio, C., Corigliano, S., Cortazzi, A., Merlo, M., 2018. Battery modeling for microgrid design: A comparison between lithium-ion and lead acid technologies. In: SPEEDAM 2018 - Proceedings: International Symposium on Power Electronics, Electrical Drives, Automation and Motion. pp. 1215–1220. http://dx.doi.org/10.1109/SPEEDAM.2018.8445343.

Moncecchi, M., Brivio, C., Mandelli, S., Merlo, M., 2020. Battery energy storage systems in microgrids: Modeling and design criteria. Energies 13 (8), 2006. http://dx.doi.org/10.3390/EN13082006.

Murty, V.V.S.N., Kumar, A., 2020. Multi-objective energy management in microgrids with hybrid energy sources and battery energy storage systems. Prot. Control Mod. Power Syst. 5 (1), 1–20. http://dx.doi.org/10.1186/S41601-019-0147-Z/TABLES/5.

Nicolosi, F.F., Alberizzi, J.C., Caligiuri, C., Renzi, M., 2021. Unit commitment optimization of a micro-grid with a MILP algorithm: Role of the emissions, bio-fuels and power generation technology. Energy Rep. 7, 8639–8651. http://dx.doi.org/10.1016/J.EGYR.2021.04.020.

Rodríguez del Nozal, A., Tapia, A., Alvarado-Barrios, L., Reina, D.G., 2020. Application of Genetic Algorithms for Unit Commitment and Economic Dispatch Problems in Microgrids. In: Studies in Computational Intelligence, vol. SCI 871, pp. 139–167. http://dx.doi.org/10.1007/978-3-030-33820-6_6.

Pan, J., Liu, T., 2022. Optimal scheduling for unit commitment with electric vehicles and uncertainty of renewable energy sources. Energy Rep. 8, 13023–13036. http://dx.doi.org/10.1016/J.EGYR.2022.09.087.

Premkumar, M., Jangir, P., Ramakrishnan, C., Nalinipriya, G., Alhelou, H.H., Kumar, B.S., 2021a. Identification of solar photovoltaic model parameters using an improved gradient-based optimization algorithm with chaotic drifts. IEEE Access 9, 62347–62379. http://dx.doi.org/10.1109/ACCESS.2021.3073821.

Premkumar, M., Jangir, P., Sowmya, R., Elavarasan, R.M., Kumar, B.S., 2021b. Enhanced chaotic JAYA algorithm for parameter estimation of photovoltaic cell/modules. ISA Trans. 116, 139–166. http://dx.doi.org/10.1016/j.isatra.2021.01.045.

Premkumar, M., Sowmya, R., 2019. An effective maximum power point tracker for partially shaded solar photovoltaic systems. Energy Rep. 5, 1445–1462. http://dx.doi.org/10.1016/j.egyr.2019.10.006.

Premkumar, M., Sowmya, R., Umashankar, S., Jangir, P., 2021. Extraction of uncertain parameters of single-diode photovoltaic module using hybrid particle swarm optimization and grey wolf optimization algorithm. Mater. Today Proc. 46, 5315–5321. http://dx.doi.org/10.1016/J.MATPR.2020.08.784.

Rezaee Jordehi, A., 2020a. A mixed binary-continuous particle swarm optimisation algorithm for unit commitment in microgrids considering uncertainties and emissions. Int. Trans. Electr. Energy Syst. 30 (11), e12581. http://dx.doi.org/10.1002/2050-7038.12581.

Rezaee Jordehi, A., 2020b. A mixed binary-continuous particle swarm optimisation algorithm for unit commitment in microgrids considering uncertainties and emissions. Int. Trans. Electr. Energy Syst. 30 (11), http://dx.doi.org/10.1002/2050-7038.12581.

Rezaee Jordehi, A., 2020c. Particle swarm optimisation with opposition learning-based strategy: an efficient optimisation algorithm for day-ahead scheduling and reconfiguration in active distribution systems. Soft Comput. 24 (24), 18573–18590. http://dx.doi.org/10.1007/S00500-020-05093-2.

Rezaee Jordehi, A., 2021a. Dynamic environmental-economic load dispatch in grid-connected microgrids with demand response programs considering the uncertainties of demand, renewable generation and market price. Int. J. Numer. Modelling, Electron. Netw. Devices Fields 34 (1), http://dx.doi.org/10.1002/JNM.2798.

Rezaee Jordehi, A., 2021b. An improved particle swarm optimisation for unit commitment in microgrids with battery energy storage systems considering battery degradation and uncertainties. Int. J. Energy Res. 45 (1), 727–744. http://dx.doi.org/10.1002/ER.5867.

Rezaee Jordehi, A., Jasni, J., 2013. Parameter selection in particle swarm optimisation: a survey. 25 (4), 527–542. http://dx.doi.org/10.1080/0952813X.2013.782348.

Sayed, A., et al., 2021. A hybrid optimization algorithm for solving of the unit commitment problem considering uncertainty of the load demand. Energies 14 (23), 8014. http://dx.doi.org/10.3390/EN14238014.

Shi, Y., Eberhart, R.C., 1998. Parameter selection in particle swarm optimization. In: Lecture Notes in Computer Science (Including Subseries Lecture Notes in Artificial Intelligence and Lecture Notes in Bioinformatics), Vol. 1447. pp. 591–600. http://dx.doi.org/10.1007/BFB0040810.

Sufyan, M., Rahim, N.A., Tan, C.K., Muhammad, M.A., Raihan, S.R.S., 2019. Optimal sizing and energy scheduling of isolated microgrid considering the battery lifetime degradation. PLoS One 14 (2), e0211642. http://dx.doi.org/10.1371/JOURNAL.PONE.0211642.

Sun, C., Zhao, H., Wang, Y., 2011. A comparative analysis of PSO, HPSO, and HPSO-TVAC for data clustering. 23 (1), 51–62. http://dx.doi.org/10.1080/0952813X.2010.506287.

Tiwari, S., Dwivedi, B., Dave, M.P., 2018. A multi-stage hybrid artificial intelligence based optimal solution for energy storage integrated mixed generation unit commitment problem. J. Intell. Fuzzy Systems 35 (5), 4909–4919. http://dx.doi.org/10.3233/JIFS-169775.

Tiwari, S., Dwivedi, B., Dave, M.P., Shrivastava, A., Agrawal, A., Bhadoria, V.S., 2021. Unit commitment problem in renewable integrated environment with storage: A review. Int. Trans. Electr. Energy Syst. 31 (10), e12775. http://dx.doi.org/10.1002/2050-7038.12775.

Trivedi, I.N., Jangir, P., Bhoye, M., Jangir, N., 2016. An economic load dispatch and multiple environmental dispatch problem solution with microgrids using interior search algorithm. Neural Comput. Appl. 30 (7), 2173–2189. http://dx.doi.org/10.1007/S00521-016-2795-5.

Wang, Z., Wang, L., Li, Z., Cheng, X., Li, Q., 2021. Optimal distributed transaction of multiple microgrids in grid-connected and islanded modes considering unit commitment scheme. Int. J. Electr. Power Energy Syst. 132, 107146. http://dx.doi.org/10.1016/J.IJEPES.2021.107146.

Xu, J., Ma, Y., Li, K., Li, Z., 2021. Unit commitment of power system with large-scale wind power considering multi time scale flexibility contribution of demand response. Energy Rep. 7, 342–352. http://dx.doi.org/10.1016/J.EGYR.2021.10.025.

Zhu, X., Zhao, S., Yang, Z., Zhang, N., Xu, X., 2022. A parallel meta-heuristic method for solving large scale unit commitment considering the integration of new energy sectors. Energy 238, 121829. http://dx.doi.org/10.1016/J.ENERGY.2021.121829.